Supplementary Materials (SM)

MOF@chitosan composites with potential antifouling properties for open-environment applications of metal-organic frameworks

Christian Jansen[a], Nam Michael Tran-Cong[b], Carsten Schlüsener[a], Alexa Schmitz[a], Peter Proksch[b], Christoph Janiak[a,]*

[a]*Institut für Anorganische Chemie und Strukturchemie, Heinrich-Heine-Universität, D-40204, Düsseldorf, Germany. *E-Mail: Janiak@hhu.de*
[b]*Institut für Pharmazeutische Biologie und Biotechnologie, Heinrich-Heine-Universität, D-40204, Düsseldorf, Germany*

Emails:

Christian.Jansen@hhu.de, Nam.Tran-Cong@hhu.de, Carsten.Schluesener@hhu.de, alexa.schmitz@hhu.de, Proksch@uni-duesseldorf.de, Janiak@hhu.de

Keywords

Metal-Organic frameworks, Al-MOFs, Chitosan, Aluminum fumarate, MIL-160, Anti-Fouling, *Chaetomium globosum*, *Aspergillus falconensis*

Table of Contents

S1. Materials and equipment

All chemicals were used as received by the supplier (*cf.* Table S1).

Table S1: Used chemicals, supplier and purities.

Chemical	**CAS number:**	**Supplier**	**Purity [%]**
Acetic acid	64-19-7	VWR Chemical	99.9
Acetone	67-64-1	VWR Chemical	p.a.
Agar	9002-18-0	Alfa Aesar	not specified
Aluminum chloride hexahydrate	7784-13-6	Fluka	not specified
Aluminum fumarate (Basolite® A520)	not specified	BASF	not specified
Chitosan medium molecular weight	9012-76-4	Sigma Aldrich	not specified
Dipotassium phosphate	7758-11-4	Merck	p.a.
Ethanol	64-17-5	Chem Solute	p.a.
Ethanol	64-17-5	Riedel de Haën	p.a.
Glutaraldehyde	111-30-8	Alfa Aesar	25 aq.
Iron(II) sulfate heptahydrate	7782-63-0	Grüssing	99.5
Monopotassium phosphate	7778-77-0	Appli Chem	p.a.
Magnesium sulfate heptahydrate	10034-99-8	Merck	p.a.
Methanol	67-56-1	Fischer Chemical	p.a.
Mowiol 20-98 (PVA) M_w~125.000	9002-89-5	Sigma Aldrich	not specified
N,N-Dimethylformamide	68-12-2	Fischer Chemical	not specified
Potassium chloride	7447-40-7	Appli Chem	p.a.
Sodium hydroxide	1310-73-2	Chem Solute	not specified
Sodium nitrate	7631-99-4	Appli Chem	p.a.
Sodium triphosphate	7758-29-4	Alfa Aesar	not specified
Silikophen® P50/X	not specified	Evonik	not specified
Tween80	9005-65-6	Sigma Aldrich	not specified
Xylene	1330-20-7	Fischer Chemical	p.a.
2,5-Furandicarboxylic acid	3238-40-2	Sigma Aldrich	not specified

Basolite® A520; Aluminum fumarate (Alfum)

Aluminum fumarate was first described in the patent literature in 2013 [1,2]. It was the first MOF synthesized on a ton scale and it is marketed by BASF under the name *Basolite® A520*. Figure S1 shows the structural features of Alfum.

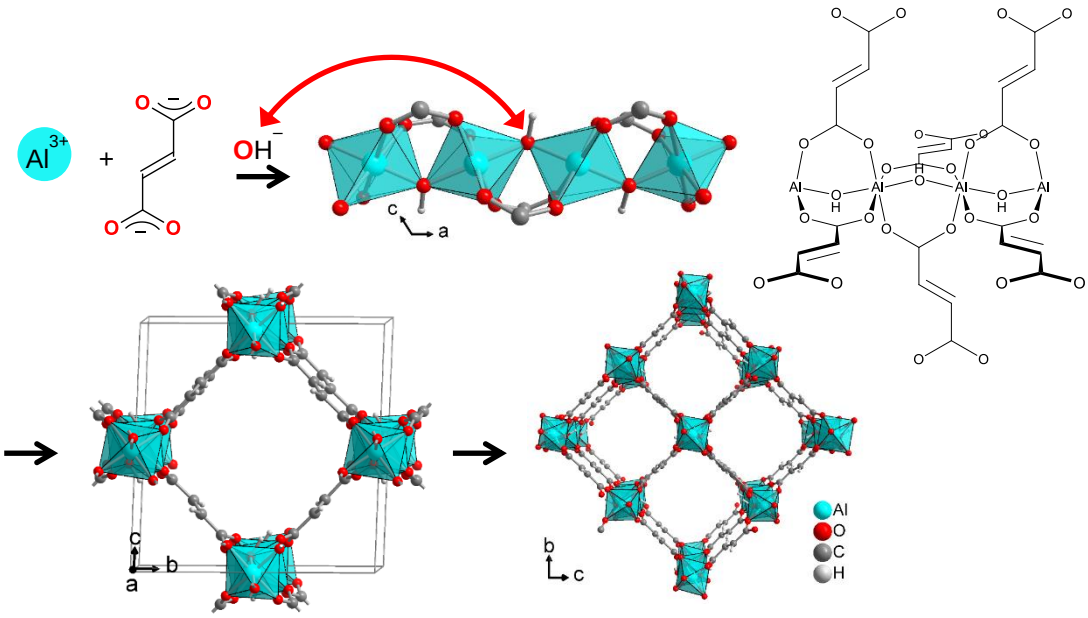

Figure S1: Al^{3+}, hydroxide and fumarate building blocks of Alfum, which give a chain of trans-µ-OH-connected vertex-bridged {AlO_6} octahedra. These chains run along the crystallographic a direction and are connected through the fumarate linkers along the bc diagonals. Graphic produced by software Diamond [3] from cif-file for Basolite A520 (CSD-Refcode DOYBEA) [4].

MIL-160

MIL-160 (*Matériaux Institut Lavoisier*) was described by Cadiau *et al.* in 2015 [5]. The MOF was obtained under reflux conditions from aqueous solutions of 2,5-furandicarboxylic acid, sodium hydroxide and aluminum chloride. MIL-160 is constructed by cis-μ-OH-connected, vertex-sharing {AlO_6} octahedra, that form helical chains, which are then joined by the linker 2,5-furandicarboxylate (Figure S2).

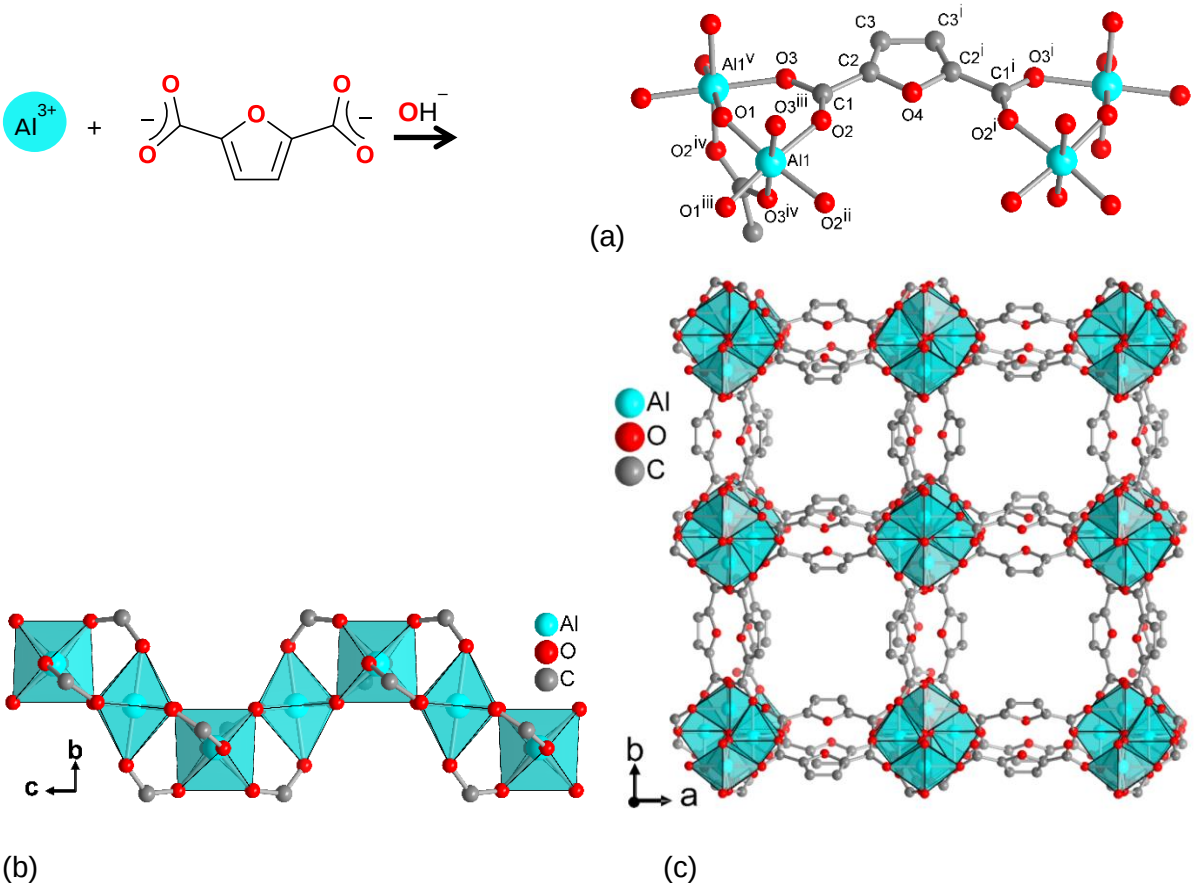

Figure S2: Structural elements in the framework of MIL-160: (a) Extended asymmetric unit with full Al coordination spheres and full ligand bridging mode. Symmetry transformations i = 1–x, y, z; ii = x, –y, –z; iii = 0.25+y, 0.25–x, –0.25+z; iv = 0.25+y, –0.25+x, 0.25–z; v = 0.25–y, –0.25+x, 0.25+z. (b) Helical chains of cis vertex-bridged {AlO_6}-polyhedra and (c) surrounded by the carboxylates ligands, to yield square-shaped one dimensional channels. Graphic produced by software Diamond [3] from cif-file for MIL-160 (CSD-Refcode PIBZOS) [6].

S2. MOF and Chitosan Synthesis

MIL-160 synthesis

Table S2: Overview MIL-160 synthesis.

Approach	Yield [%]	BET Surface [m^2 g^{-1}]
MIL-160	66	1186

Chitosan syntheses

Table S3: Overview of the crosslinked chitosan syntheses.

Chitosan concentration [g L^{-1}]	Chitosan [g]	2 wt-% acetic acid [mL]	BET surface [m^2 g^{-1}]
Crosslinked with $Na_5P_3O_{10}$			
6	0.3	50	144
20	0.4	20	230
30	0.6	20	220
40	0.4	10	202
Crosslinked with Glutaraldehyde			
6	0.04	6.66	233

Chitosan synthesis in glutaraldehyde

A chitosan solution with 6 g L^{-1} was prepared with 2 wt-%acetic acid. The solution was transferred to a truncated syringe (5 mL) and glutaraldehyde (25 % in water, 1 mL, 83 g L^{-1} final concentration) added under vigorous stirring. As soon as a slight gelation occurred, the stirrer was quickly removed. The syringe was closed and the gel aged (RT, 72 h). The resulting gel was gently pushed out of the syringe into Milli-Q water and washed (24 h). It was then dehydrated in ethanol (at least 6 d). The resulting monolith was dried by supercritical CO_2.

S3 Composite Synthesis

Table S4: Comparison of the composite materials and the educts. (d. s. = dried supercritically)

Educt/Composite materials	**Chitosan conc. [g L^{-1}]**	**BET-surface [m^2 g^{-1}]**	
		measured	**calculated**
Alfum	-	988	-
Alfum60@chitosan	6	20	650
Alfum60@chitosan	20	294	685
Alfum80@chitosan	6	474	819
Alfum80@chitosan	20	587	836
Alfum80@chitosan d. s.	6	844	819
Alfum80@chitosan d. s.	20	893	836
Alfum90@chitosan	6	964	904
Alfum90@chitosan	20	856	912
Alfum60@chitosan	30	202	681
Alfum60@chitosan	40	26	674
Alfum60@chitosan with glutaraldehyde	6	697	686
MIL-160	-	1186	-
MIL-160(60)@chitosan	6	32	769
MIL-160(60)@chitosan	20	138	804
MIL-160(80)@chitosan	6	720	978
MIL-160(80)@chitosan	20	610	995
MIL-160(80)@chitosan d. s.	6	858	978
MIL-160(80)@chitosan d. s.	20	918	995
MIL-160(90)@chitosan	6	1068	1082
MIL-160(90)@chitosan	20	964	1090
Alfum@PVA	-	716	-
MIL-160@PVA	-	925	-
Alfum pressed	-	759	988
Alfum pressed with Silikophen®	-	257	988
MIL-160 pressed	-	726	1126
MIL-160 pressed with Silikophen®	-	479	1126

MOF@Silikophen composites (pressure calculation)

$$Surface = \pi * r^2 = \pi * (0.0065\ m)^2 = 1.33 * 10^{-4} m^2 \quad \textbf{(S1)}$$

$$Force = mass * acceleration = 2000\ kg * 9.81 \frac{m}{s^2} = 19620 \frac{kg*m}{s^2} \quad \textbf{(S2)}$$

$$Pressure = \frac{force}{surface} = \frac{19620 \frac{k*m}{s^2}}{1.33*10^{-4} m^2} = 147518797\ Pa = 1475.2\ bar \quad \textbf{(S3)}$$

Alfum@chitosan synthesis in glutaraldehyde

A chitosan solution with 6 g L^{-1} was prepared with 2 wt-%acetic acid. Then 40 mg Alfum were added to 2 mL of the solution and stirred for 30 minutes. The suspension was transferred to a truncated syringe (5 mL) and glutaraldehyde (25 % in water, 1 mL, 83 g L^{-1} final concentration) was added under vigorous stirring. As soon as a slight gelation occurred, the stirrer was quickly removed. The syringe was closed and the gel aged (RT, 72 h). The resulting gel was gently pushed out of the syringe into Milli-Q water and washed (24 h). It was then dehydrated in ethanol (at least 6 d). The resulting monolith was dried by supercritical CO_2.

For PXRD see Fig. S7, for IR spectra see Fig. S12, for N_2 sorption Fig. S31, for H_2O sorption Fig. S39.

S4 Antifouling Tests

The amounts of the experiment antifouling tests are shown in the following Table S5.

Table S5: Composition of the nutrient medium in the fungi tests.

Chemical	**Amount**
Stock mineral salt solution 1.1	
$NaNO_3$	4.0 g
KH_2PO_4	1.4 g
K_2HPO_4	0.6 g
KCl	1.0 g
$MgSO_4$ * 7 H_2O	1.0 g
$FeSO_4$·* 7 H_2O	0.02 g
Reinstwasser	2000 mL
Mineral salt solution with additive 1.2	
Tween80	0.05 g auf 500 mL *1.1*
Incomplete culture medium 1.4	
Agar	20.0 g auf 1000 mL *1.1*

Table S6: Results of the antifouling tests with Chaetomium globosum and Aspergillus falconensis.

Sample	**Fungi**		
	Chaetomium globosum	*Aspergillus falconensis*	
	1. Run	1. Run	2./3. Run
Chitosan (medium molecular weight)	-	3	5
Chitosan (20 g/L)	2	0	5
Alfum60@chitosan	-	0	0
Alfum80@chitosan	5	0	0
Alfum90@chitosan	5	2	0
MIL-160(60)@chitosan	5	2	0
MIL-160(80)@chitosan	5	1	0
MIL-160(90)@chitosan	5	2	0
Alfum (Basolite® A520)	5	3	5
MIL-160	5	1	1
Alfum@PVA	5	2	3
MIL-160@PVA	1	0	2
Alfum@Silikophen®	5	5	5
MIL-160@Silikophen®	5	1	2

The evaluation of the samples was based on Method A of DIN EN ISO 846 (10/1997) (testing for resistance to fungi) [7].

S5 PXRD Measurements

Powder X-ray diffractometry (PXRD) used a *Bruker D2 Phaser* diffractometer (unless noted otherwise) with a flat silicon, low background sample holder and Cu-Kα radiation (λ = 1.54184 Å) at 30 kV and 0.0125° s^{-1} in the 2θ = 5-50 ° range, exposure time: 1 s, stepsize: 0.15 or 0.05° giving typically a total measurement time of 6 for a diffractogram.
In Figure S3 and S4, the PXRDs of the neat MOFs were also measured with a Rigaku Miniflex 600 (Rigaku, Tokio;Japan) using Cu-Kα radiation (λ = 1.54182 Å) between 5° < 2θ < 50° with a scan rate of 0.083 ° s^{-1} (600 W, 40 kV, 15 mA) and a step size of 0.01 °per step giving a total measurement time of 10 min for a diffractogram.
Figure S3 - Figure S9 depict PXRD patterns of all obtained samples.

Alfum

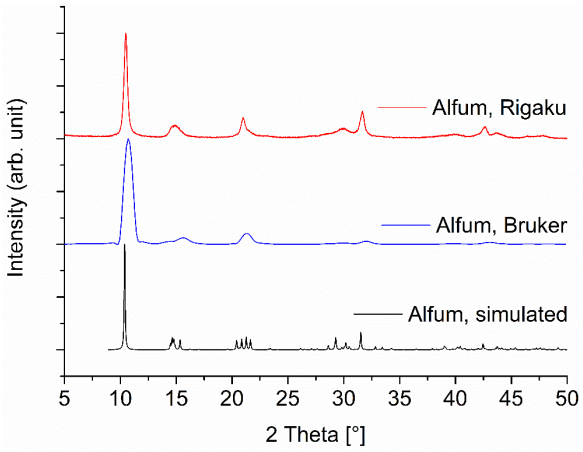

Figure S3: PXRD patterns of Alfum samples obtained by measurements of the Basolite® A520, in comparison with simulatd pattern (CSD-Refcode DOYBEA) [4]. Bruker D2 diffractometer (blue), Rigaku Miniflex diffractometer (red). The PXRD of Alfum was obtained from the purchased MOF from BASF which is less crystalline than MIL-160 (cf. Figure S4), due to the industrial scale of its synthesis.

MIL-160

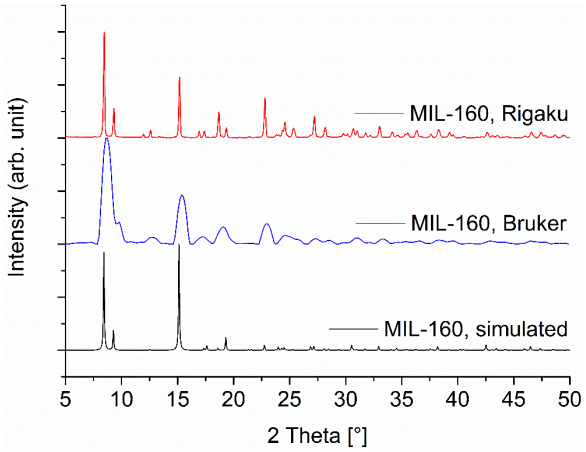

Figure S4: PXRD pattern of MIL-160 obtained by synthesis in comparison with simulated pattern (CSD-Refcode PIBZOS) [6]. Bruker D2 diffractometer (blue), Rigaku Miniflex diffractometer (red).

Alfum@chitosan

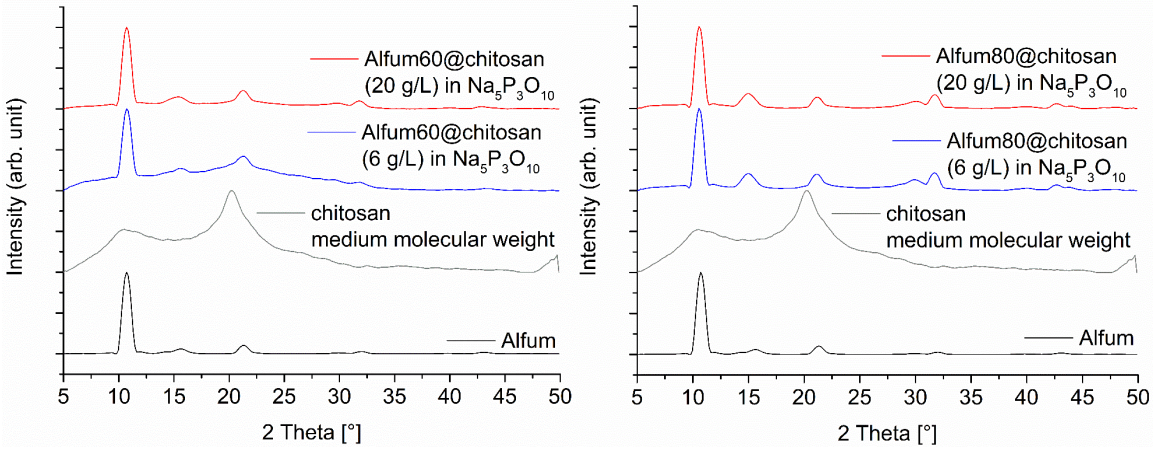

Figure S5: PXRD patterns of Alfum@chitosan composites for a MOF content of 60 wt-% (left) and 80 wt-% (right), prepared with different chitosan concentrations.

MIL-160@chitosan

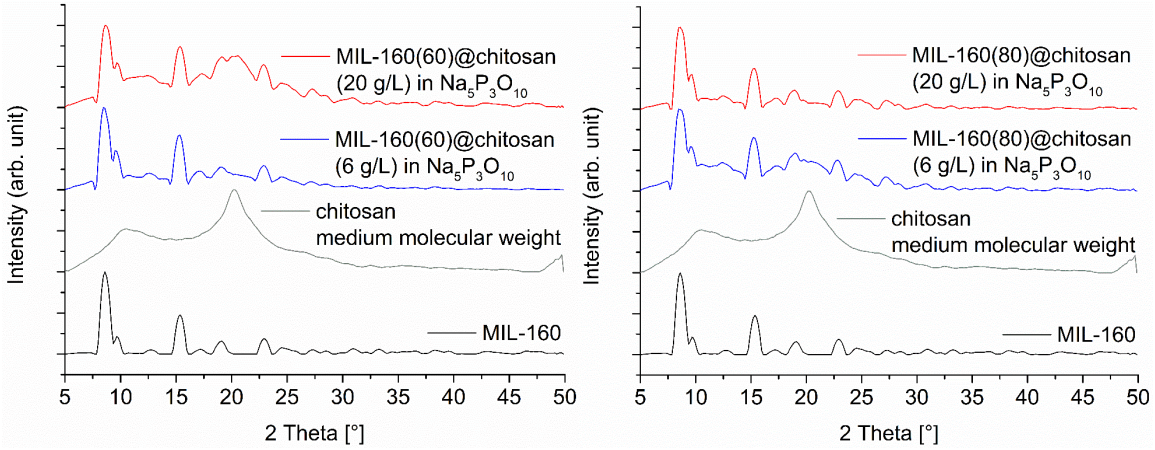

Figure S6: PXRD patterns of MIL-160@chitosan composites with different chitosan concentrations, in comparison with educts. Left: 60 wt-% MOF loading, right: 80 wt-% MOF loading.

Alfum@chitosan in glutaraldehyde

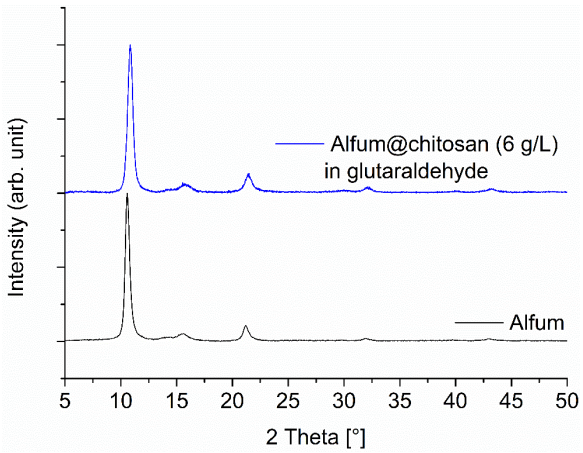

Figure S7: PXRD pattern of Alfum@chitosan in glutaraldehyde composites with chitosan, in comparison with the starting material. The diffractograms here were measured with a time of 30 min, thereby giving narrower reflections than in the other 6-minute diffractograms.

MOF@PVA

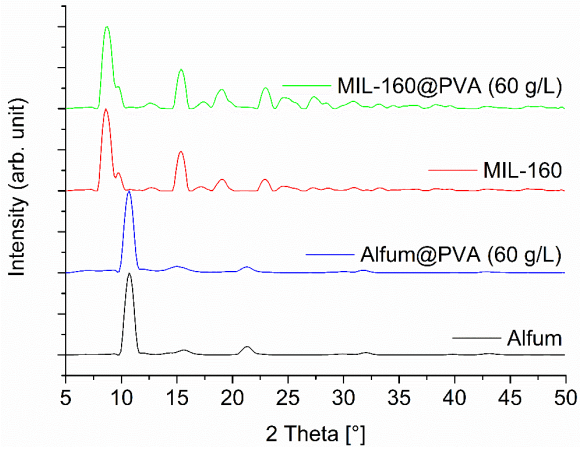

Figure S8: PXRD patterns of MOF@PVA composites, in comparison with the starting materials.

MOF@Silikophen®

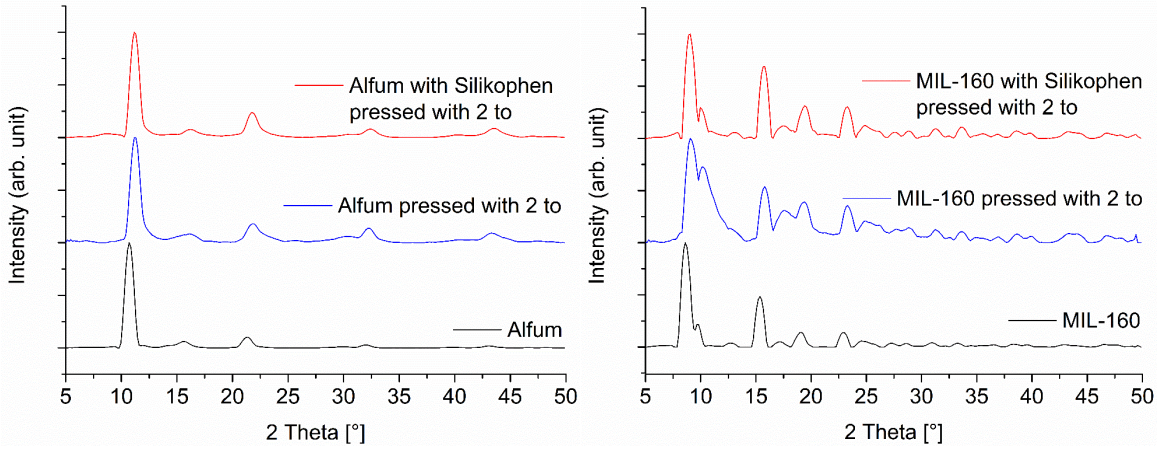

Figure S9: PXRD patterns of MOF@Silikophen® composites in comparison with starting materials and pressed starting materials. Left: Alfum, right: MIL-160 (to = tons of pressure). It can be seen, that the preparation of the pellets with a pressure of 2 tons results in a visible peak broadening which correlates with a loss of crystallinity. It is known that (porous) MOF structures are not very stable at high pressures. The preparation of pellets was necessary to perform the antifouling tests.

S6 Infrared spectra

FT-IR spectra were measured in KBr-mode on a BRUKER TENSOR 37 IR spectrometer in the range of 4000−400 cm^{-1}.

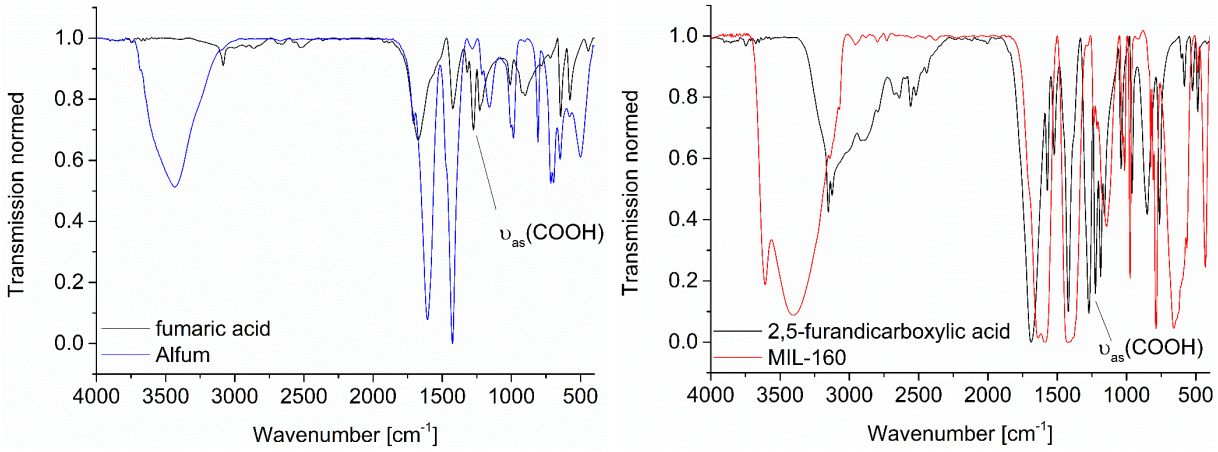

Figure S10: IR-spectra of MOFs in comparison with linker. Left: Alfum and fumaric acid, right: MIL-160 and 2,5-furandicarboxylic acid.

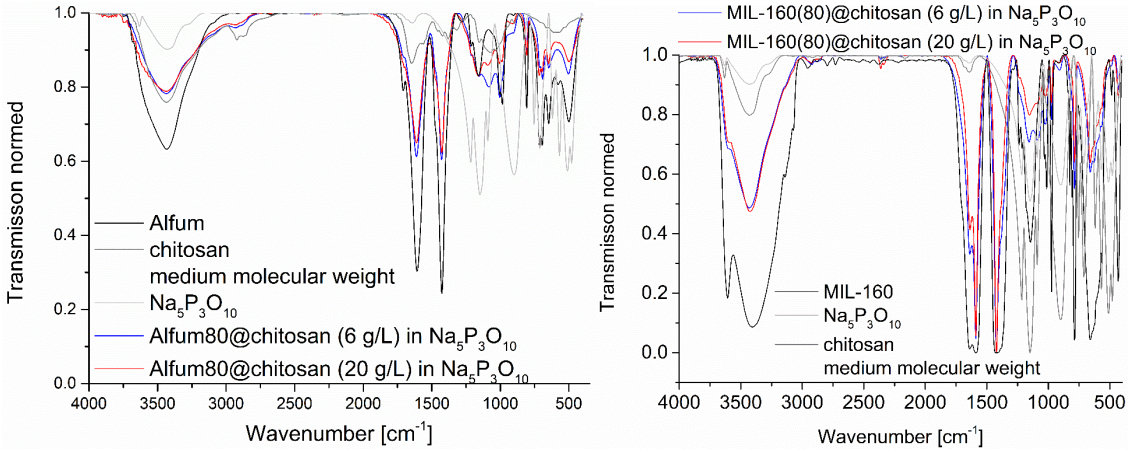

Figure S11: IR-spectra of MOF@chitosan composites with different chitosan concentrations, in comparison with educts. Left: Comppsites, Alfum, Chitosan, $Na_5P_3O_{10}$ and fumaric acid, right: Composites, MIL-160, Chitosan, $Na_5P_3O_{10}$ and 2,5-furandicarboxylic acid.

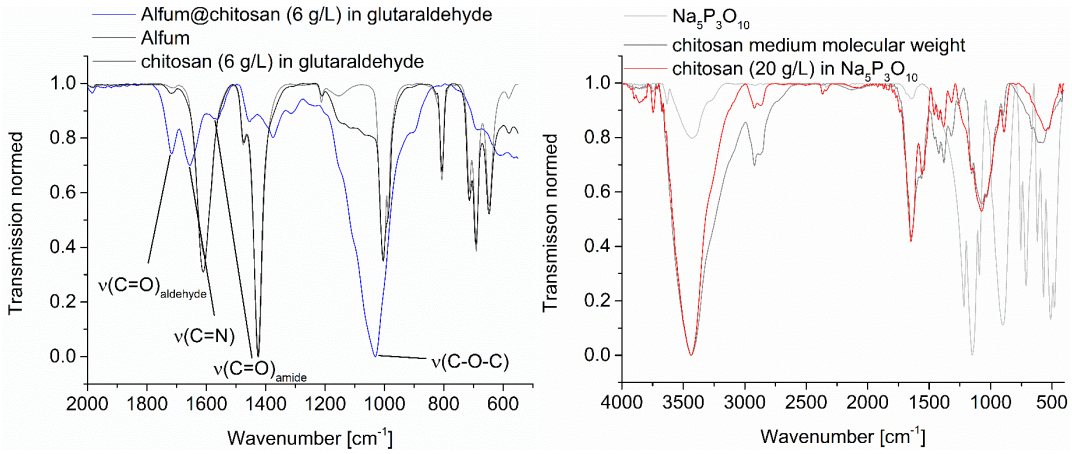

Figure S12: IR-spectra of MOF@chitosan in glutaraldehyde (left) and crosslinked Chitosan, in comparison with chitosan and $Na_5P_3O_{10}$ (right).

S7 Thermogravimetric Analysis (TGA)

Exemplarily, we performed thermogravimetric analyses (TGA) of some samples.

Figure S13 - Figure S16: TG curve of MOF@PVA composites, compared with educts.

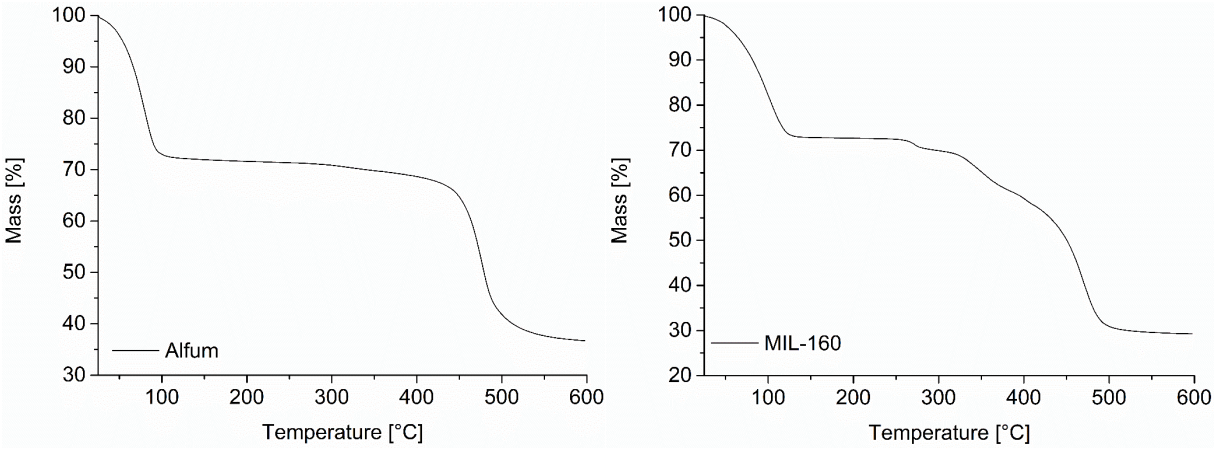

Figure S13: TG curve of Alfum (Basolite® A520) (left) and MIL-160 (right).

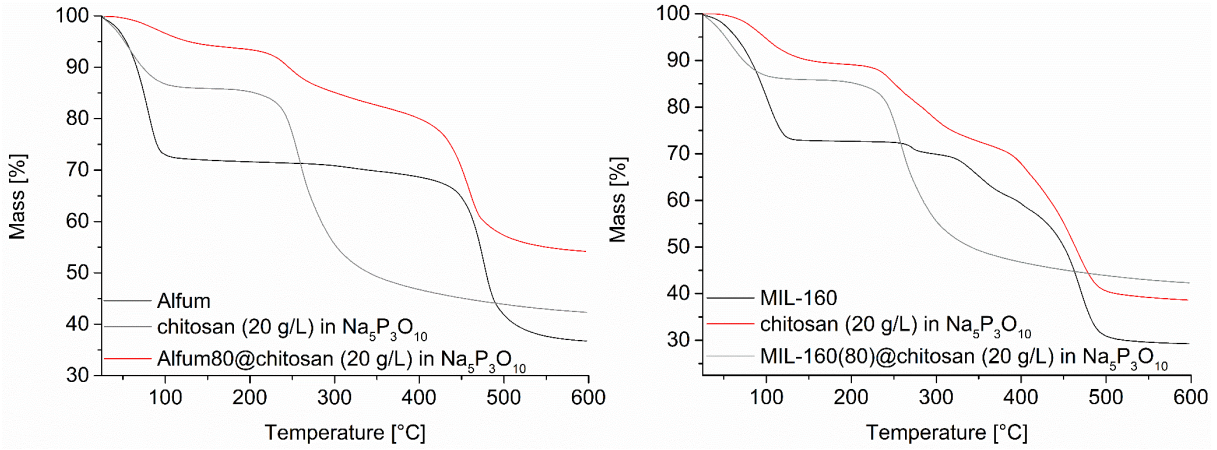

Figure S14: TG curves of MOF@chitosan curves, in comparison with MOF and crosslinked chitosan. Left: Alfum, right: MIL-160.

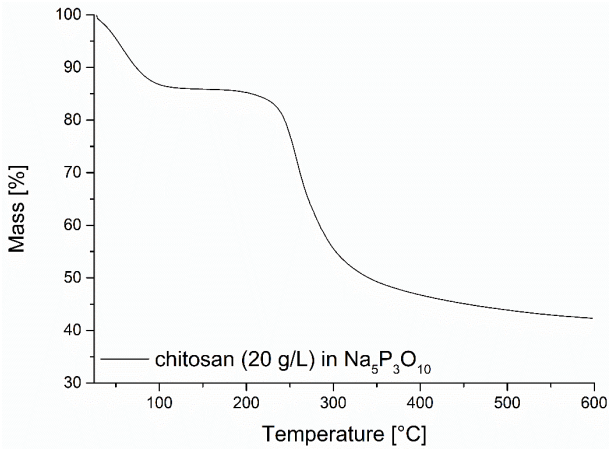

Figure S15: TG curve of crosslinked chitosan.

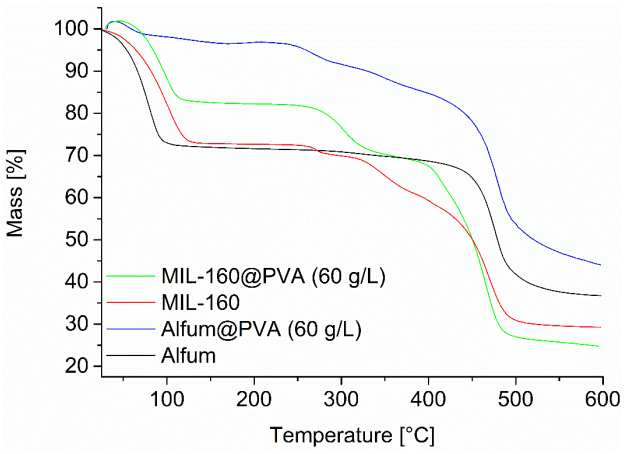

Figure S16: TG curve of MOF@PVA composites, compared with educts.

S8 Scanning electron microscopy (SEM)

For control of morphology we recorded SEM images using a *JEOL JSM-6510 advanced electron microscope* with a LaB_6 cathode at 20 keV. The microscope was equipped with a *Bruker Xflash 410 silicon drift detector* and the *Bruker ESPRIT* software for EDX analysis.
Figure S17 – Figure S25 exemplarily depict SEM images and EDX measurements of selected samples of the MOFs and MOF@Polymer composites.

Alfum

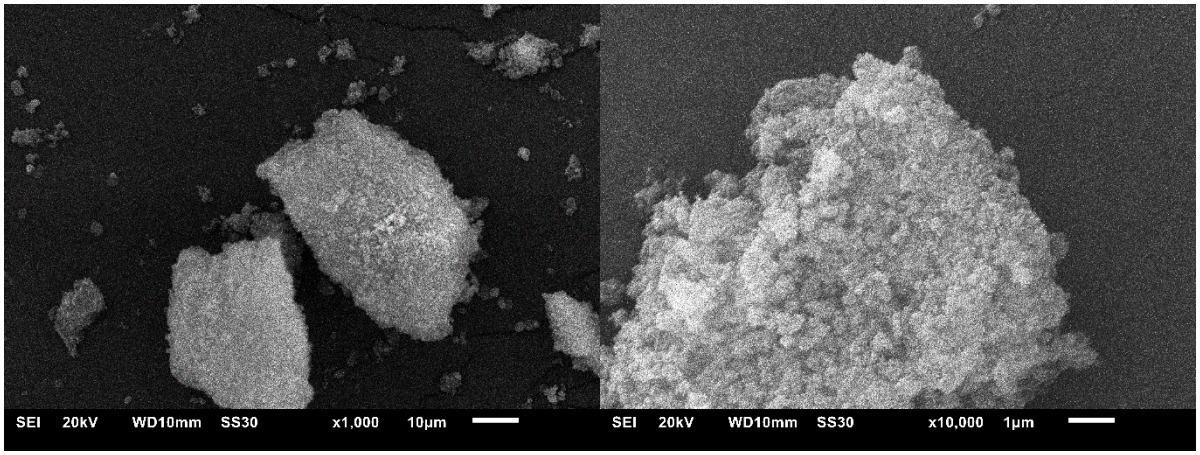

Figure S17: SEM images of Alfum at different magnifications (left: overview, right: close-up).

MIL-160

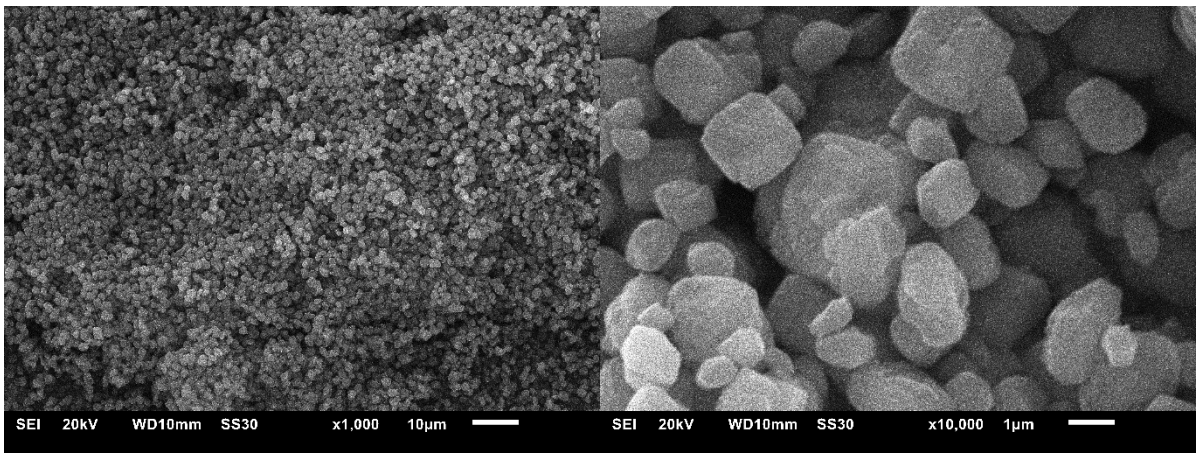

Figure S18: SEM images of MIL-160 at different magnifications (left: overview, right: close-up).

Chitosan

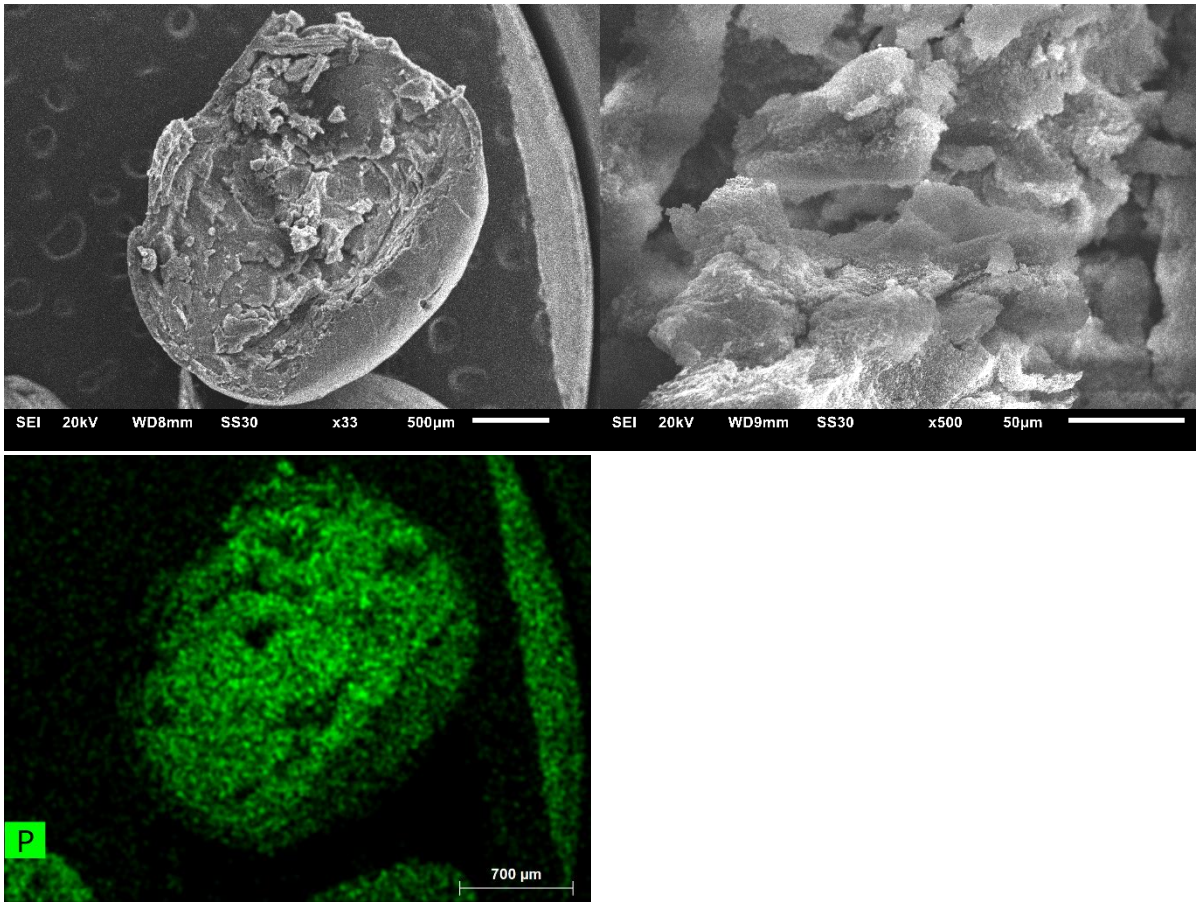

Figure S19: SEM images of chitosan at different magnifications (top left: overview, top right: close-up). EDX-element mapping for phosphorus (bottom) for the particle in the overview at top left.

Alfum@chitosan

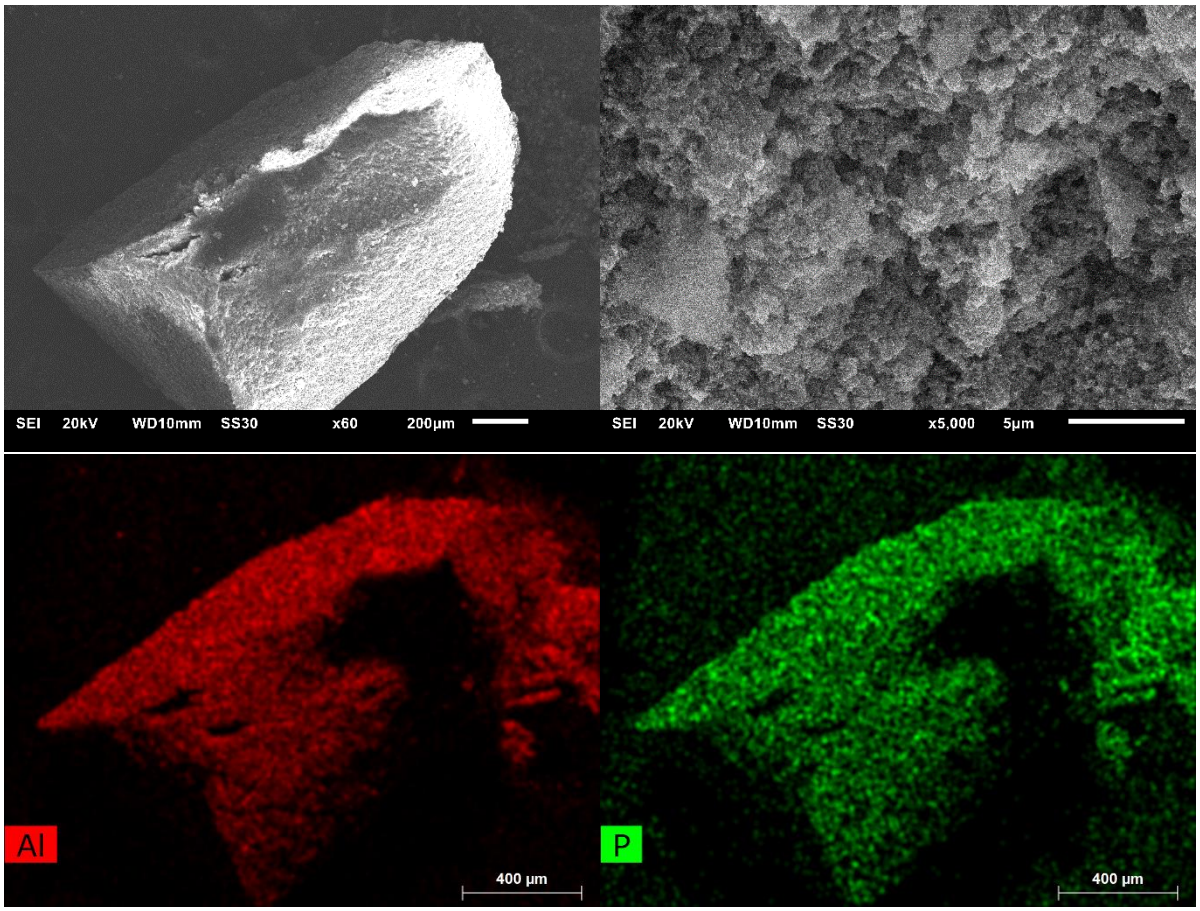

Figure S20: SEM images of Alfum90@chitosan at different magnifications (top left: overview, top right: close-up). EDX-element mapping for aluminum and phosphorus (bottom) for the particle in the overview at top left. The dark areas, that is lower amount of Al and P in the center-right of the element mapping is due to the particle geometry. The hollow in the middle of the particle causes a blocking of the emerging X-rays from the sample which then cannot be detected.

MIL-160@chitosan

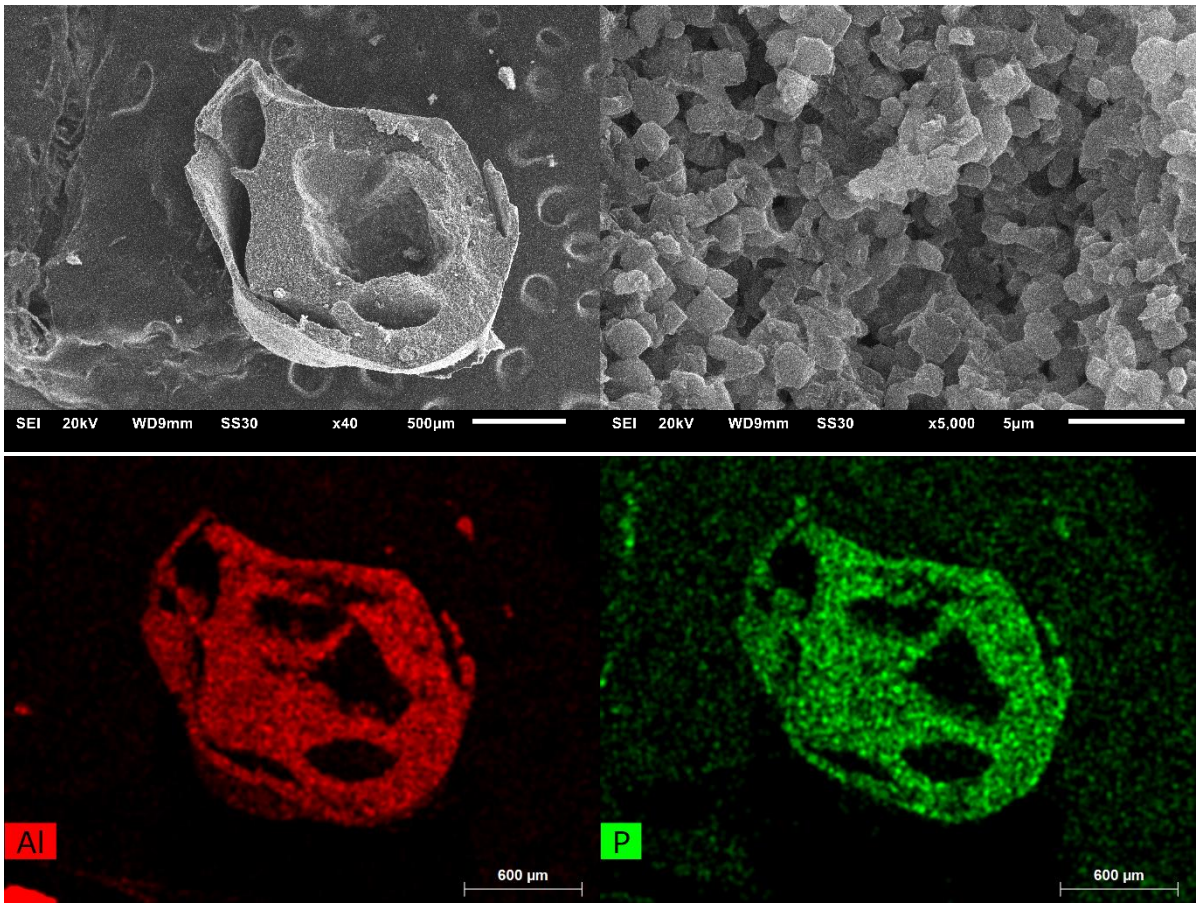

Figure S21: SEM images of MIL-160(80)@chitosan at different magnifications (top left: overview, top right: close-up). EDX-element mapping for aluminum and phosphorus (bottom) for the particle in the overview at top left. The dark features in the element maps are and artefact due to blocking of the emerging element-specific X-rays from the sample by the grooves in the bead surface so that these X-rays cannot be detected.

MOF@PVA

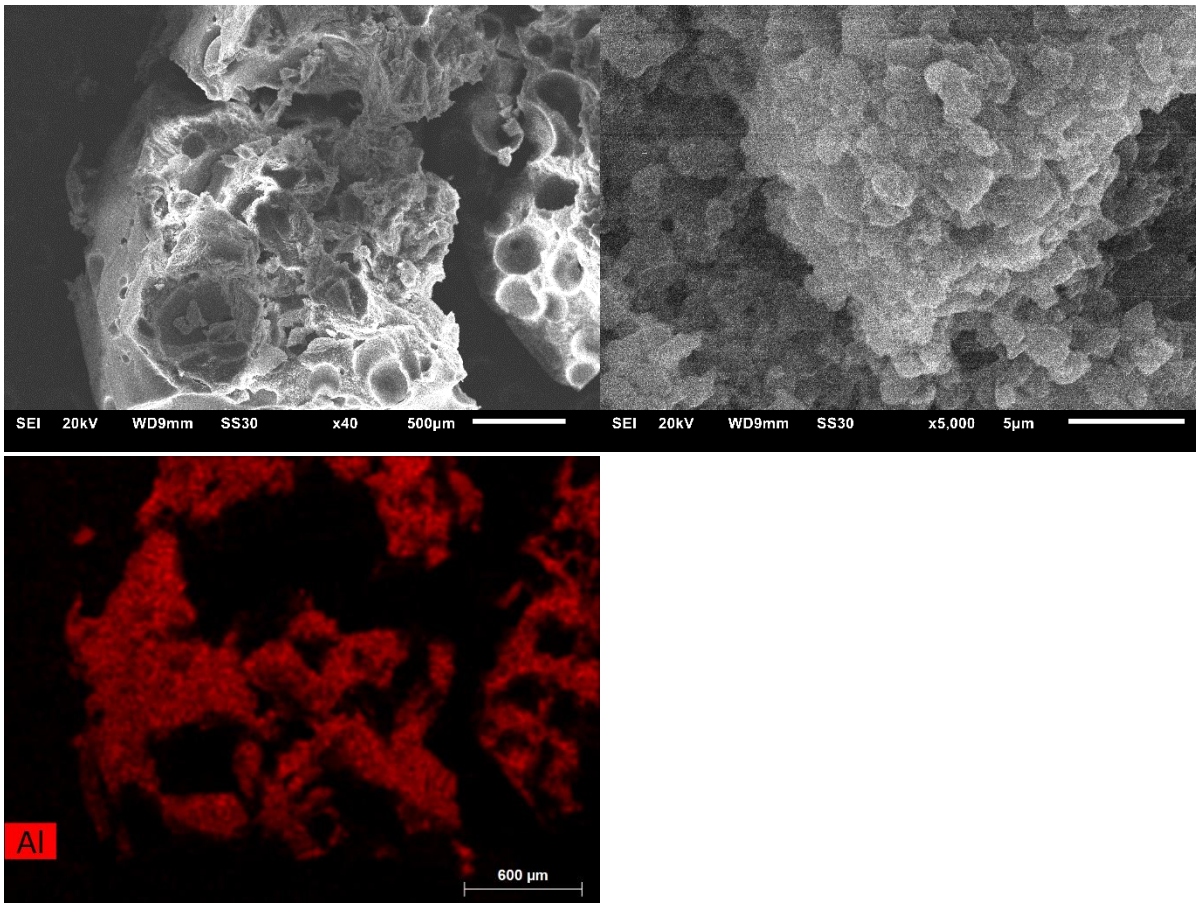

Figure S22: SEM images of Alfum80@PVA at different magnifications (top left: overview, top right: close-up). EDX-element mapping for aluminum (bottom). The dark features in the element maps are and artefact due to blocking of the emerging element-specific X-rays from the sample by the grooves in the bead surface so that these X-rays cannot be detected.

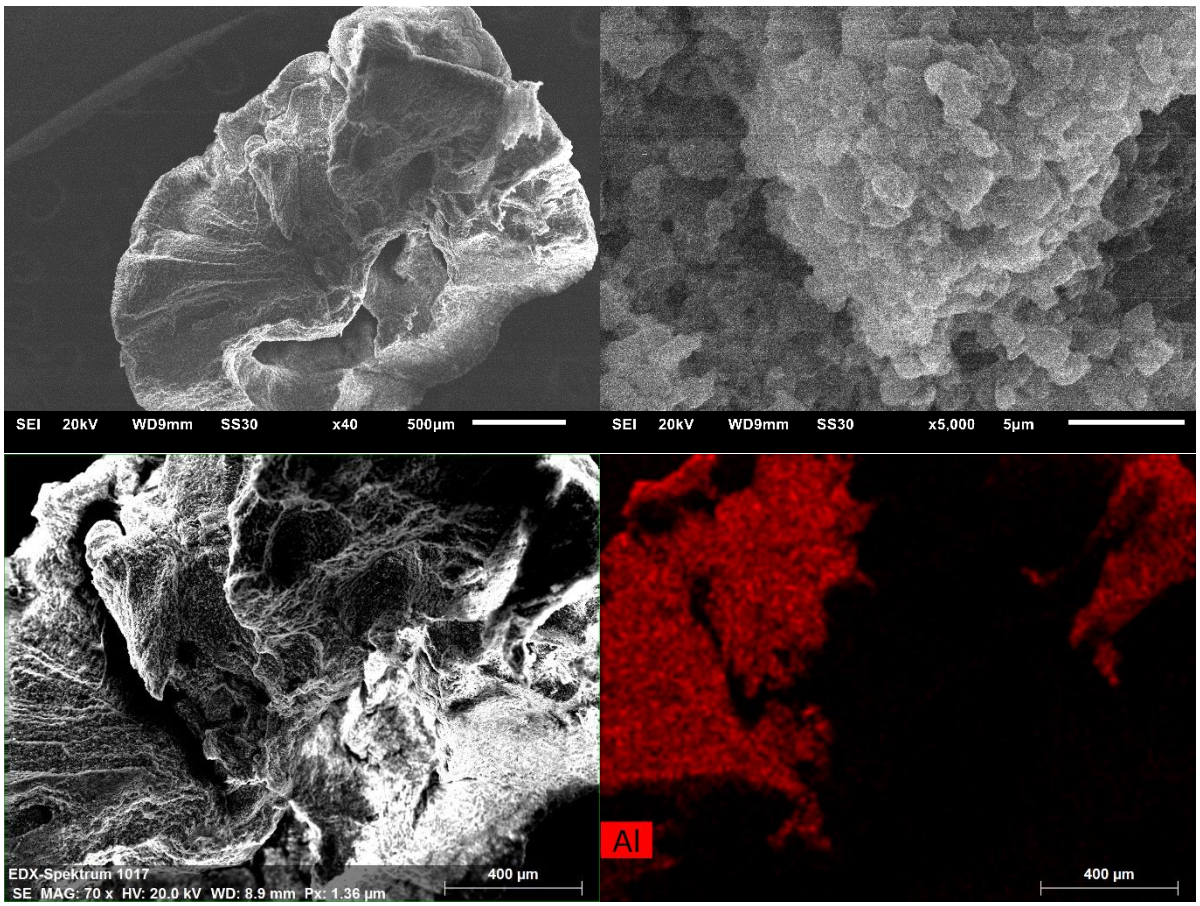

Figure S23: SEM images of MIL-160(80)@PVA at different magnifications (top left: overview, top right: close-up, bottom left: cutout from the overview). EDX-element mapping for aluminum (bottom right). The dark features in the element maps are and artefact due to blocking of the emerging element-specific X-rays from the sample by the grooves in the bead surface so that these X-rays cannot be detected.

MOF@Silikophen®

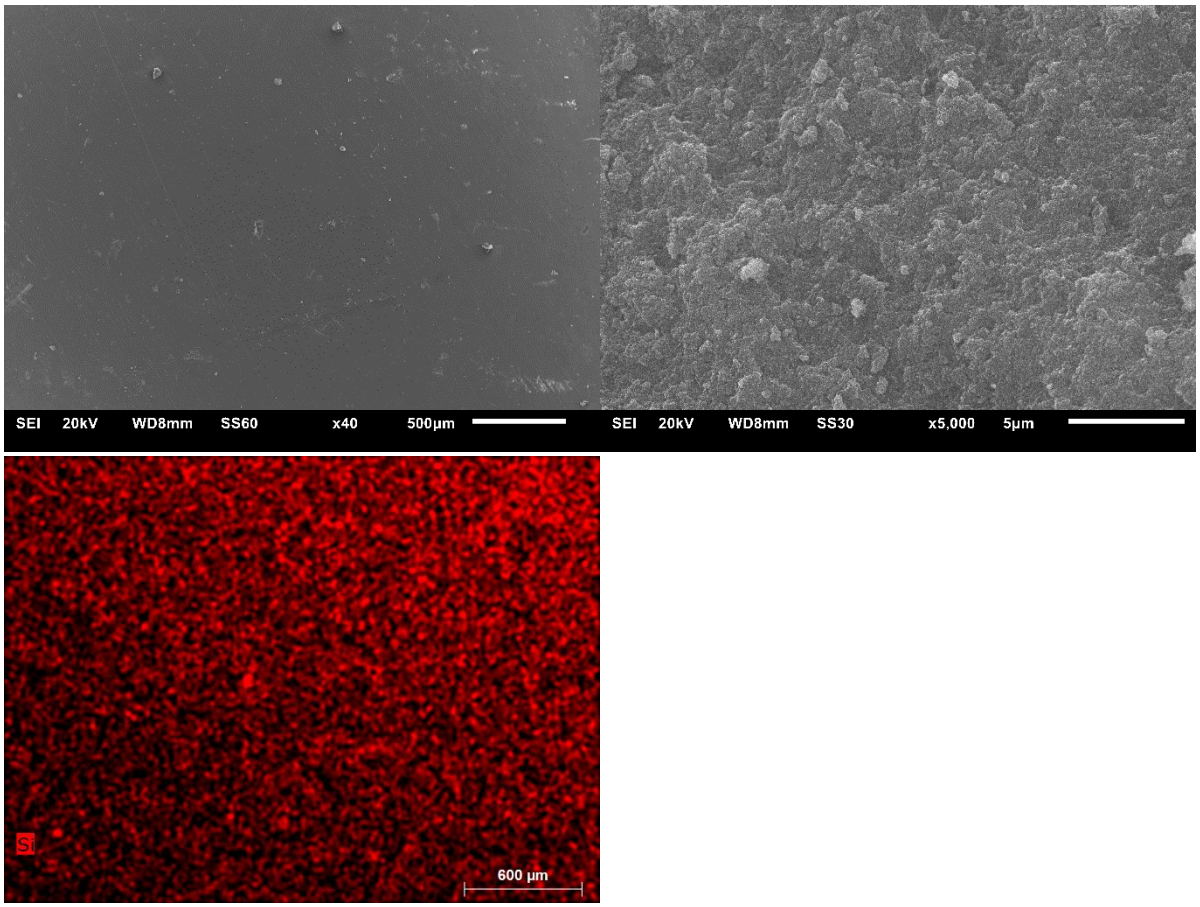

Figure S24: SEM images of Alfum80@Silikophen® at different magnifications (top left: overview, top right: close-up). EDX measurement for aluminum (bottom).

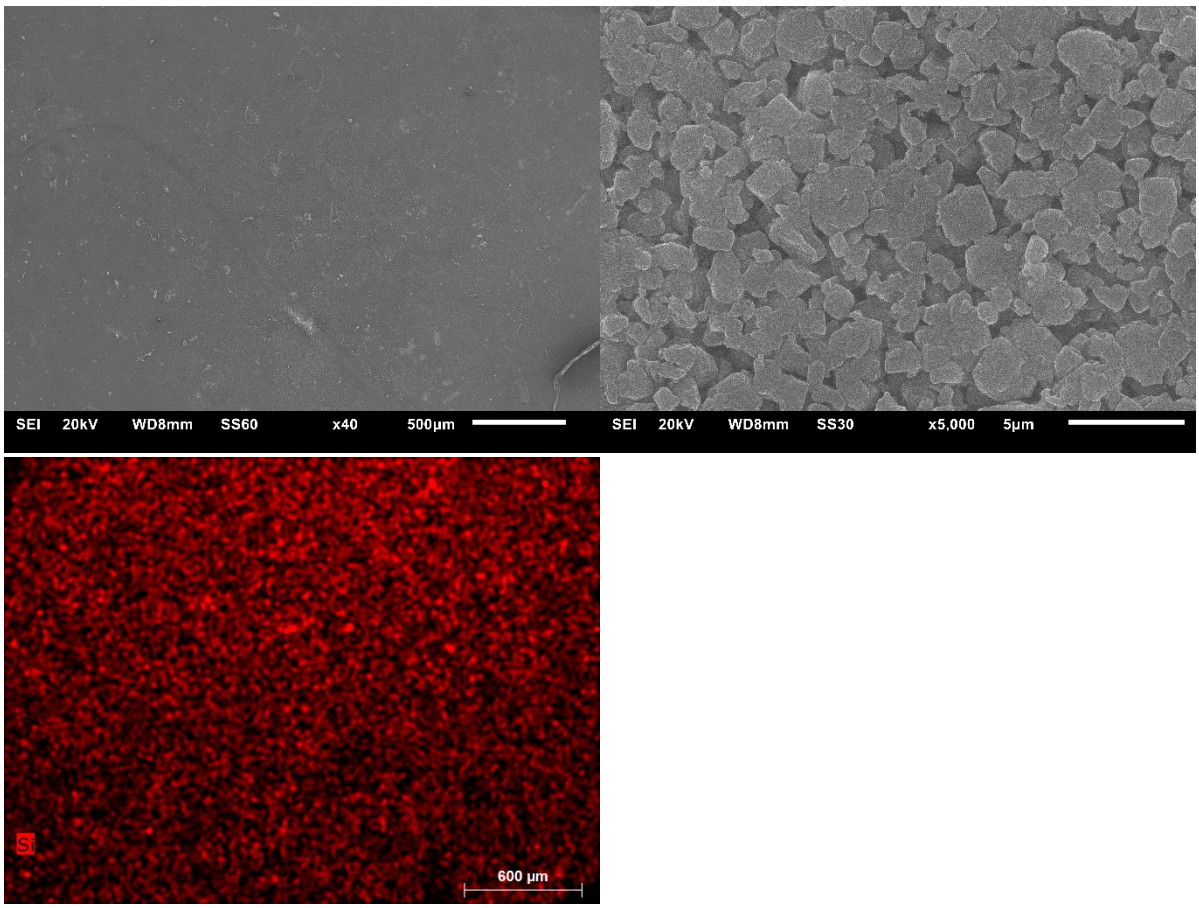

Figure S25: SEM images of MIL-160(80)@Silikophen® at different magnifications (top left: overview, top right: close-up). EDX measurement for aluminum (bottom).

S9 Nitrogen sorption experiments (T = 77 K)

Surface areas (BET) were determined by nitrogen (purity 99.999%) sorption experiments at 77.35 K using a *Quantachrome Autosorb6* instrument within a partial pressure range of p p_0^{-1} = 10–3^{-1} bar. Each sample was degassed under vacuum (< 10^{-2} mbar) at 120 °C for *ca.* 3 h, prior to measurement. All surface areas (BET) were calculated from five adsorption points in the pressure range pp_0^{-1} = 0.009 -0.041 bar for all samples. This range is indeed not recommended by IUPAC (International Union of Pure and Applied Chemistry) for BET surface determination, but rather suitable for microporous materials [8]. Figure S26 - Figure S33 depict the N_2 sorption isotherms of all samples.

Alfum

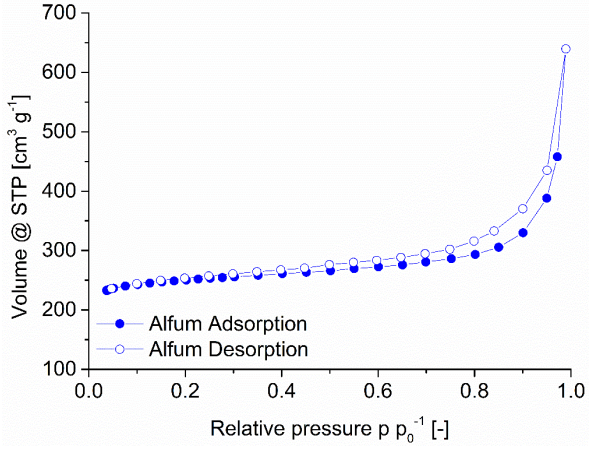

Figure S26: Nitrogen sorption (77 K) isotherm of Alfum.

MIL-160

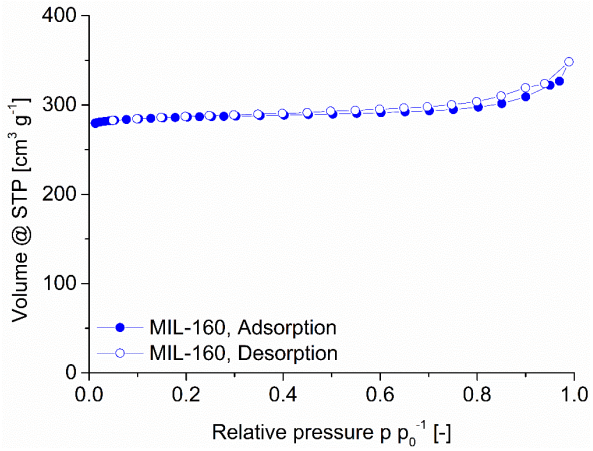

Figure S27: Nitrogen sorption (77 K) isotherms of MIL-160.

Chitosan

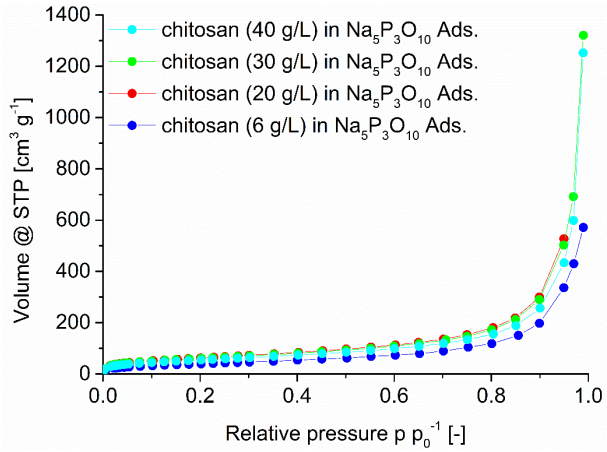

Figure S28: Nitrogen sorption (77 K) isotherm of chitosan beads with different concentrations.

Alfum@chitosan

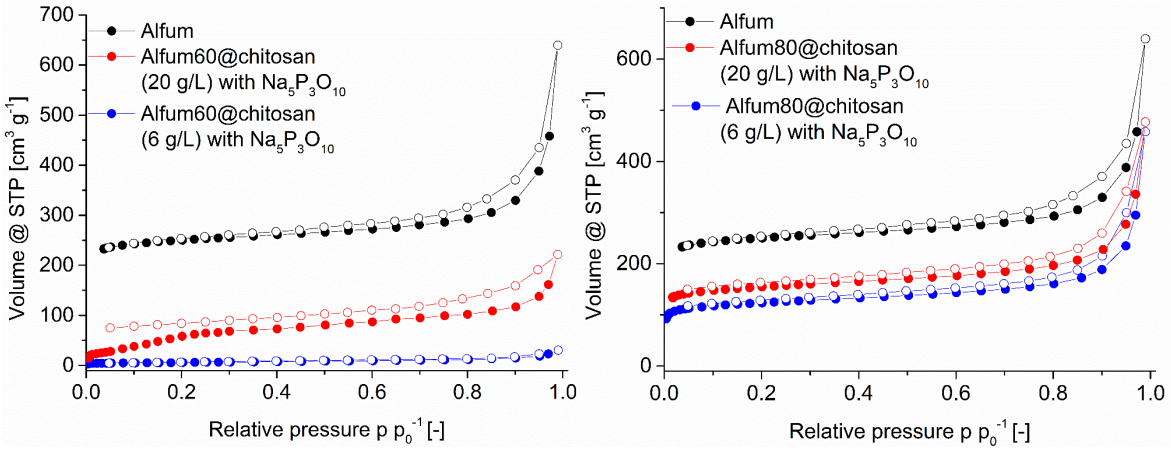

Figure S29: Nitrogen sorption (77 K) isotherm of Alfum@chitosan composites with different chitosan concentrations, in comparison with Alfum. Left: 60 wt-% MOF loading, right: 80 wt-% MOF loading.

MIL-160@chitosan

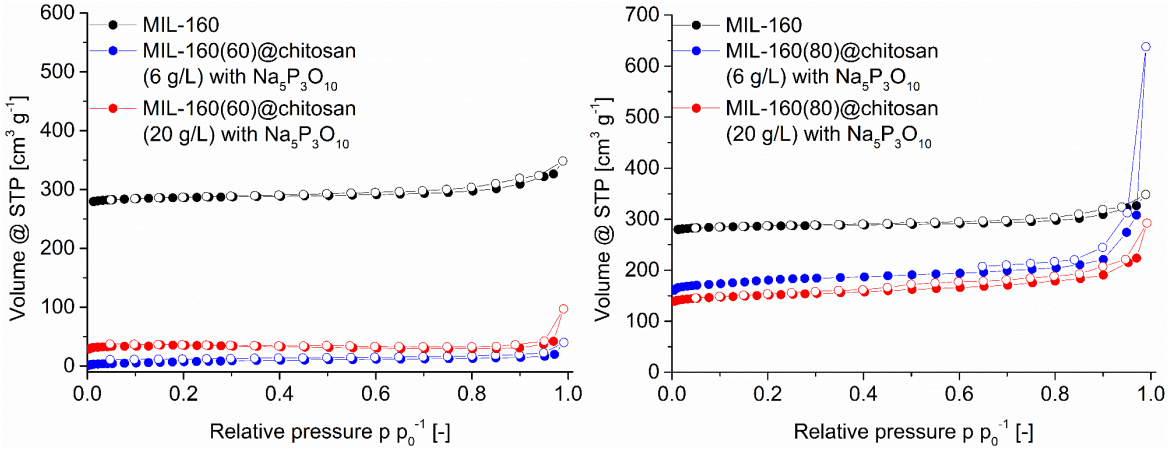

Figure S30: Nitrogen sorption (77 K) isotherm of MIL-160@chitosan composites with different chitosan concentrations, in comparison with MIL-160. Left: 60 wt-% MOF loading, right: 80 wt-% MOF loading.

Alfum@chitosan in glutaraldehyde

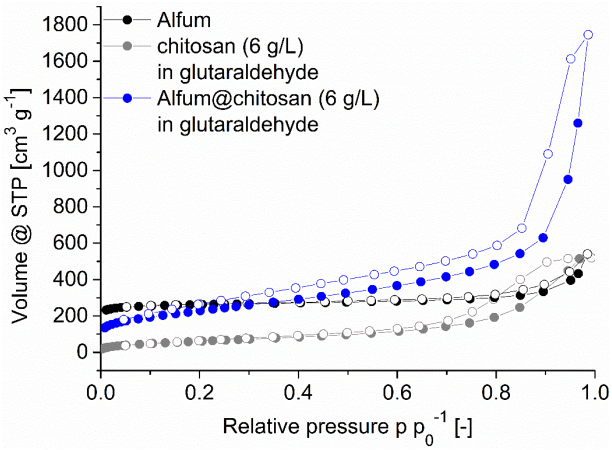

Figure S31: Nitrogen sorption (77 K) isotherm of Alfum@chitosan in glutaraldehyde composites with chitosan, in comparison with Alfum.

MOF@PVA

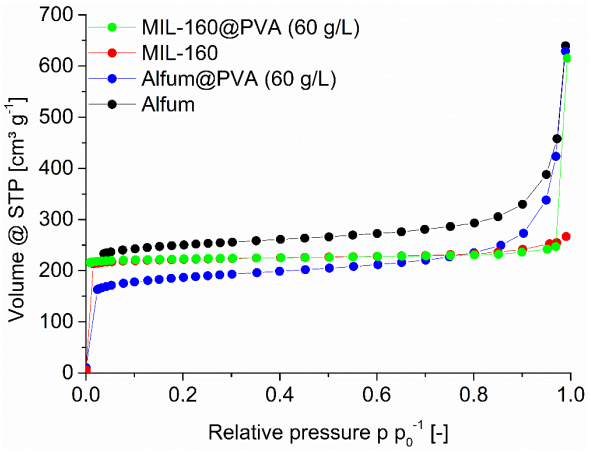

Figure S32: Nitrogen sorption (77 K) isotherms of MOF@PVA composites, in comparison with MOFs. Only adsorption is shown.

MOF@Silikophen®

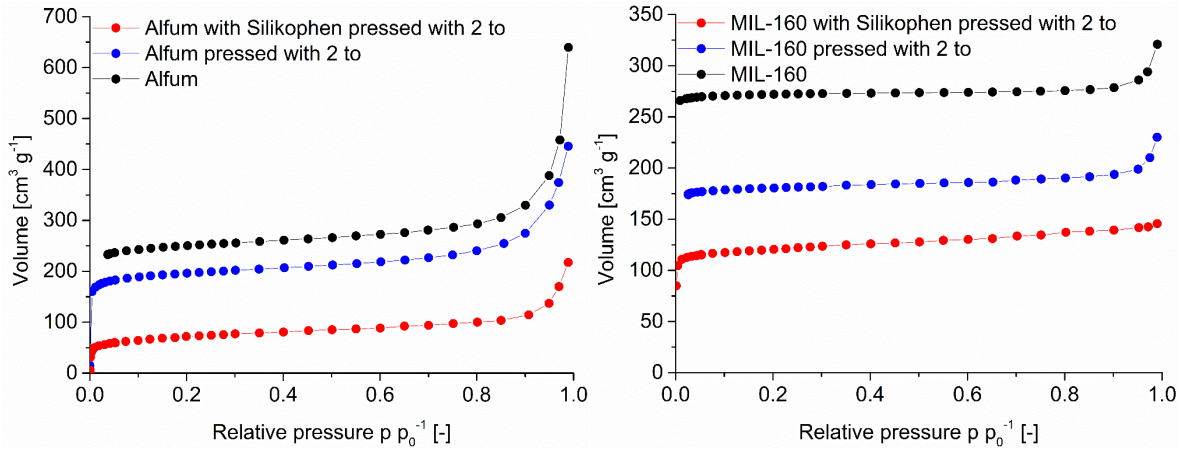

Figure S33: Nitrogen sorption (77 K) isotherms of MOF@Silikophen® composites, in comparison with MOFs and pressed MOFs. Only adsorption is shown.

S10 Water sorption experiments (T = 293 K)

Water sorption experiments were carried out on a *Quantachrome VStar4* (QUANTACHROME, Odelzhausen, Germany) instrument within a partial pressure range of $pp0^{-1}$ = 10–3^{-1} bar. Each sample was degassed under vacuum (< 10^{-3} mbar) at 120 °C for *ca.* 3 h prior to measurement, using a *FloVac* (QUANTACHROME, Odelzhausen, Germany) degasser.

Figure S34 - Figure S40 depict water sorption isotherms of all obtained samples.

Alfum

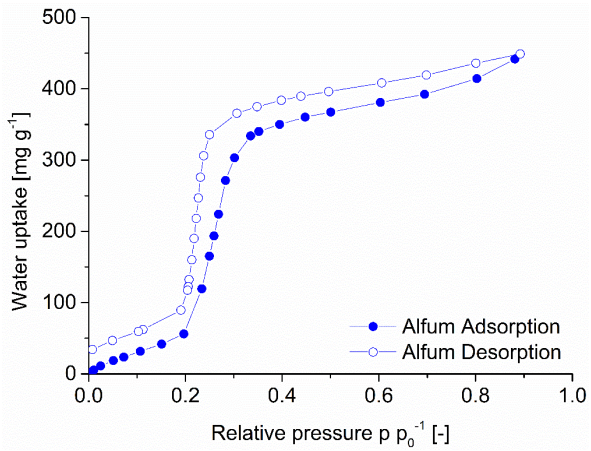

Figure S34: Water sorption (293 K) isotherm of Alfum.

MIL-160

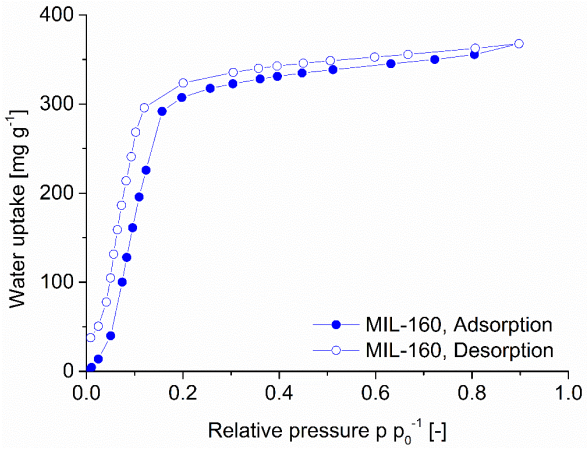

Figure S35: Water sorption (293 K) isotherms of MIL-160.

Chitosan

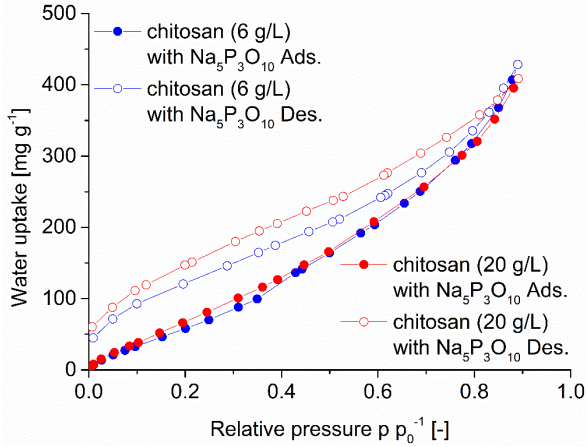

Figure S36: Water sorption (293 K) isotherms of chitosan beads with different concentrations.

Alfum@chitosan

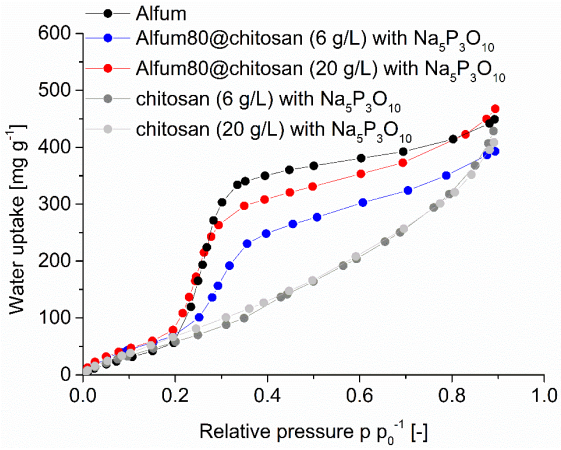

Figure S37: Water sorption (293 K) isotherms of Alfum80@chitosan composites with different chitosan concentrations, in comparison with Alfum and crosslinked chitosan.

MIL-160@chitosan

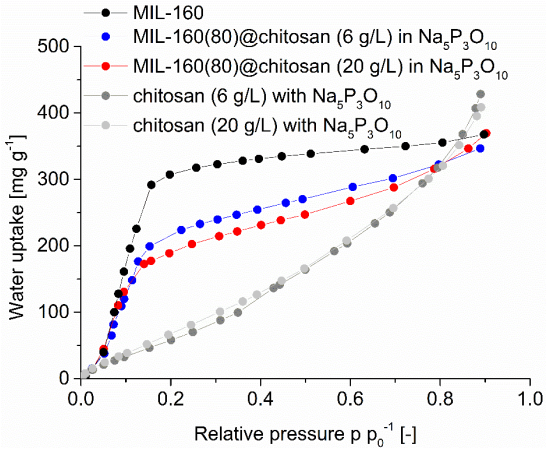

Figure S38: Water sorption (293 K) isotherms of MIL-160(80)@chitosan composites with different chitosan concentrations, in comparison with MIL-160 and crosslinked chitosan.

Alfum@chitosan in glutaraldehyde

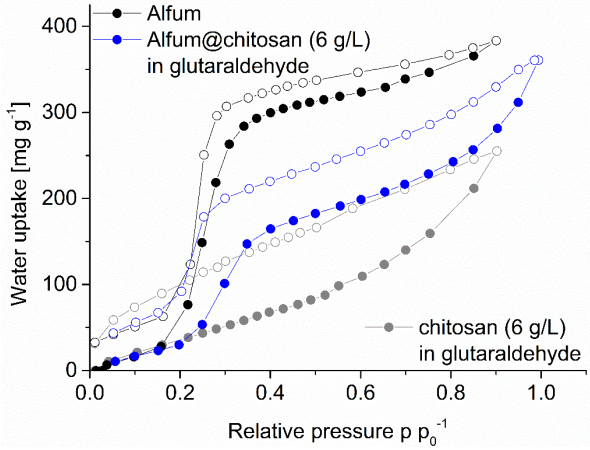

Figure S39: Water sorption (293 K) isotherms of Alfum@chitosan in glutaraldehyde with chitosan in comparison with Alfum.

MOF@PVA

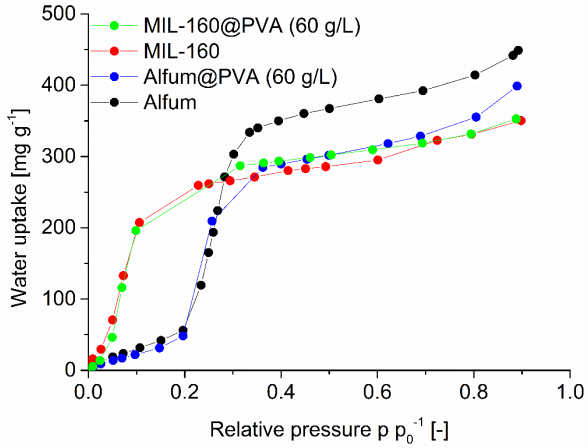

Figure S40: Water sorption (293 K) isotherms of MOF@PVA composites, in comparison with MOFs. Only adsorption is shown.

S11 Antifouling tests series (images)

Method A: *Chaetomium globosum*

Sample / Day	Chitosan	Alfum	Alfum80 @chitosan	Alfum90 @chitosan
0				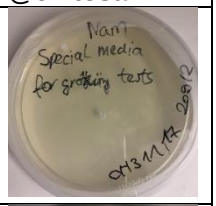
1		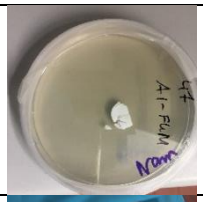	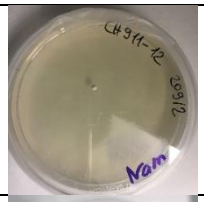	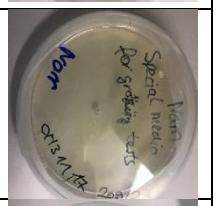
2				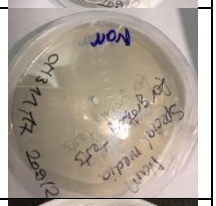
3		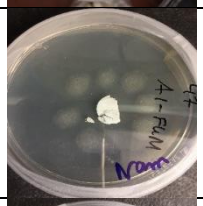	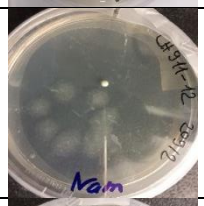	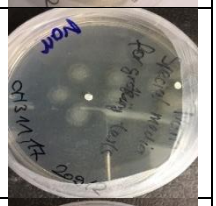
5	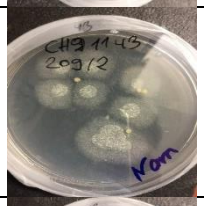	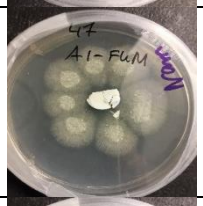	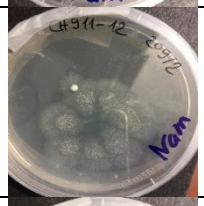	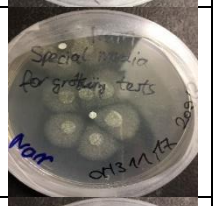
7	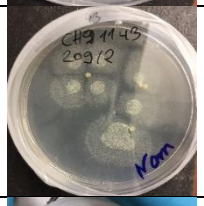	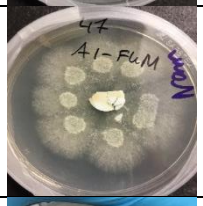	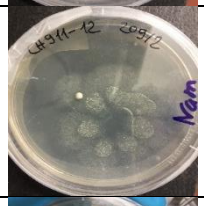	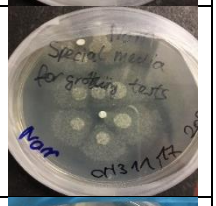
8	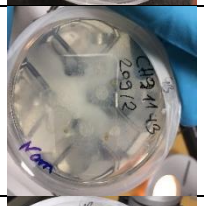	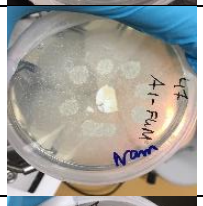		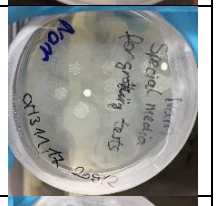
9	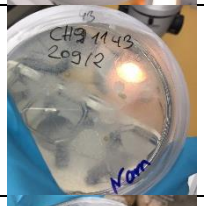		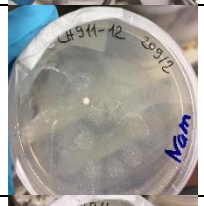	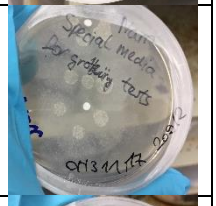
15	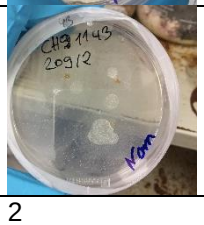	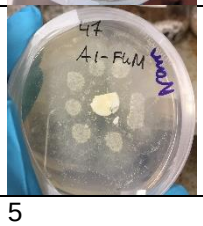	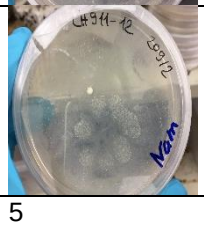	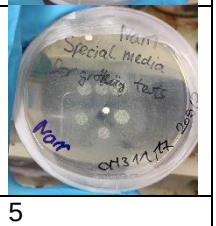
category	2	5	5	5

Sample / Day	Chitosan	MIL-160	MIL-160(60) @chitosan	MIL-160(80) @chitosan	MIL-160(90) @chitosan
0	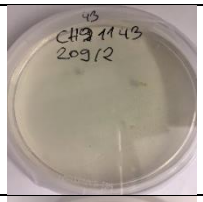		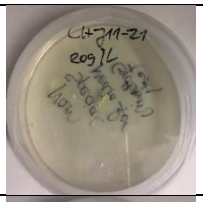		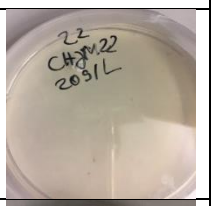
1	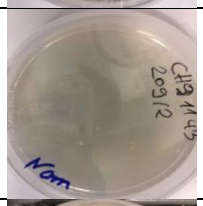	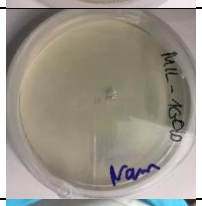	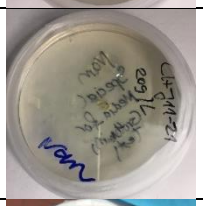		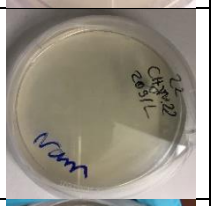
2		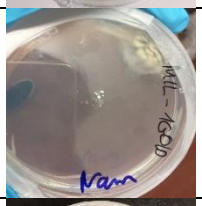	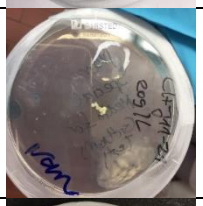	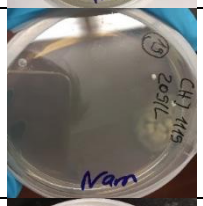	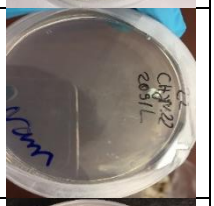
3	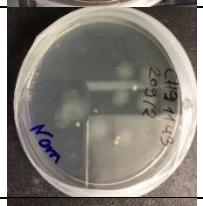	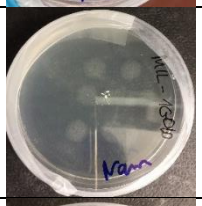			
5			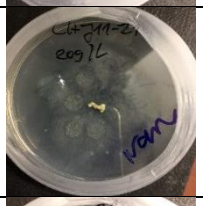	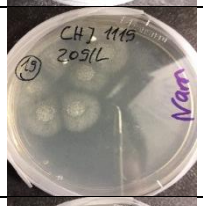	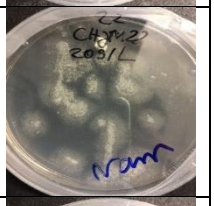
7	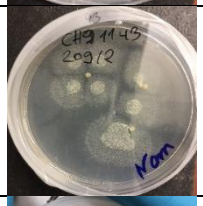	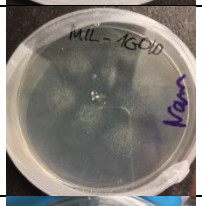	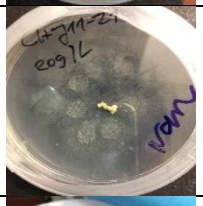	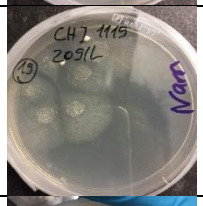	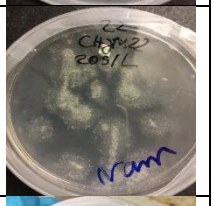
8			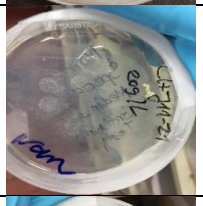		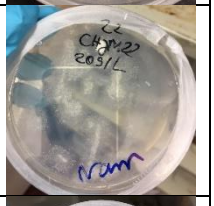
9	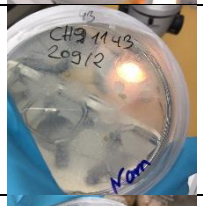	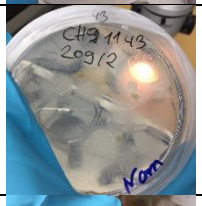	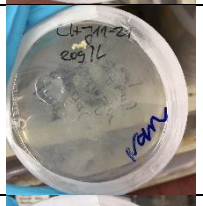	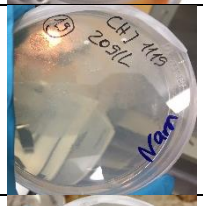	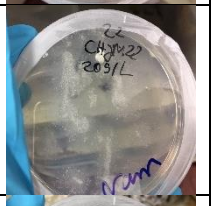
15					
category	2	5	5	5	5

Sample / Day	Alfum@PVA	MIL-160@PVA	Alfum@ Silikophen®	MIL-160@ Silikophen®
0			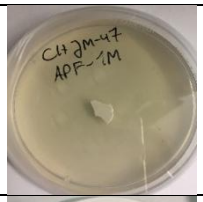	
1	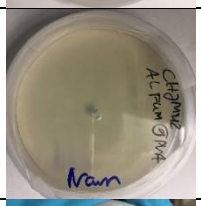		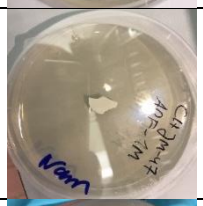	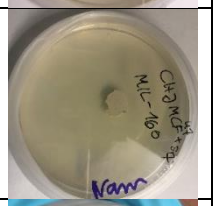
2	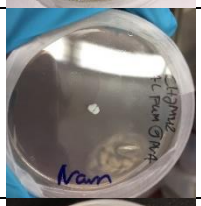	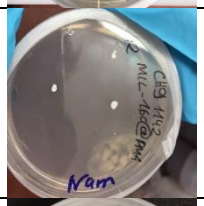	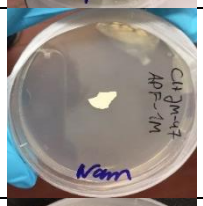	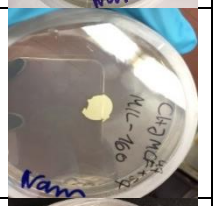
3	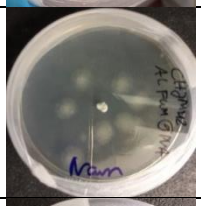			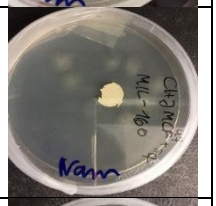
5	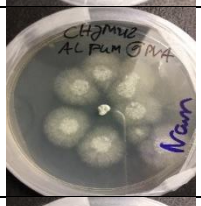	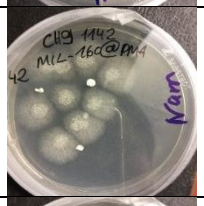		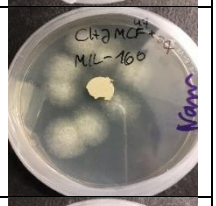
7	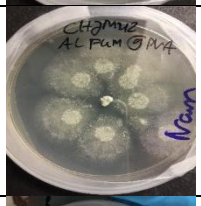	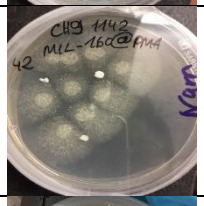		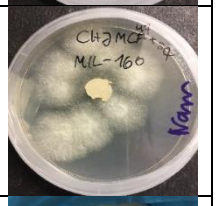
8	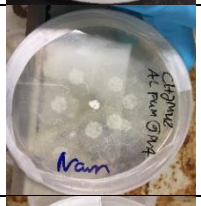	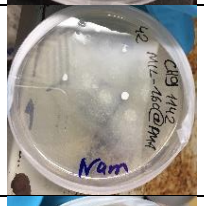		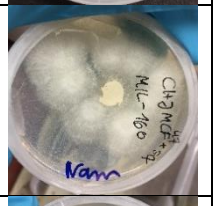
9		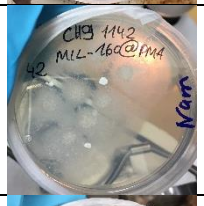		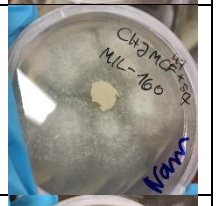
15	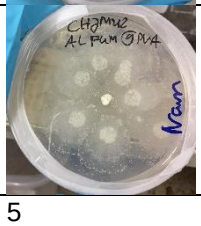	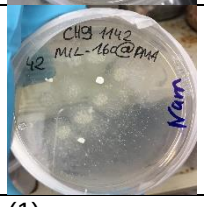	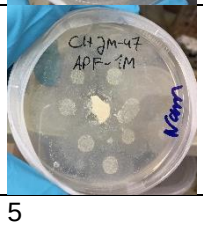	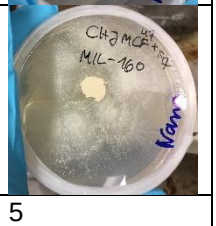
category	5	(1)	5	5

Method A: *Aspergillus falconensis* (1st Run)

Sample / Day	Chitosan	Alfum	Alfum60 @chitosan	Alfum80 @chitosan	Alfum90 @chitosan
0	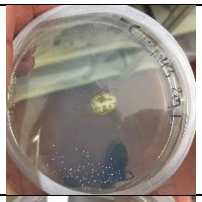				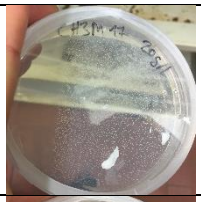
2	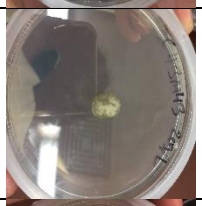	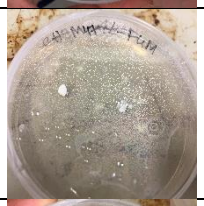			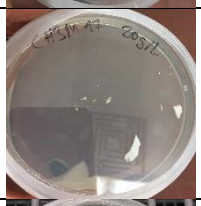
3		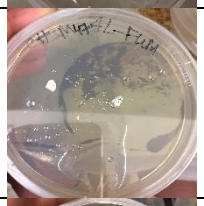		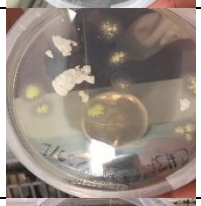	
4					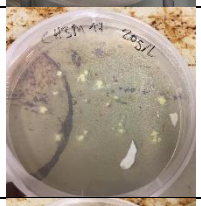
5					
6					
11				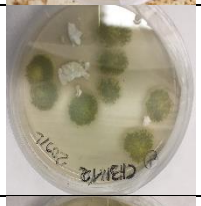	
27					
category	3	3	0	0	2

Sample / Day	Chitosan	MIL-160	MIL-160(60) @chitosan	MIL-160(80) @chitosan	MIL-160(90) @chitosan
0	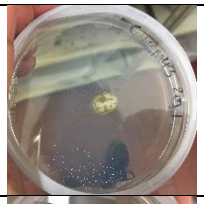	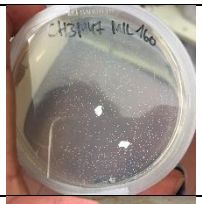			
2	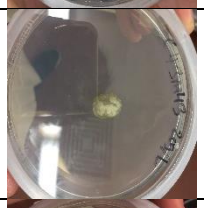			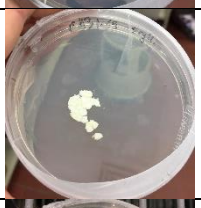	
3			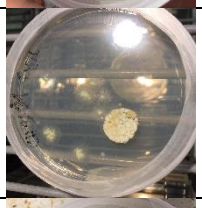		
4	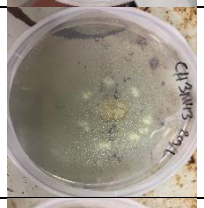	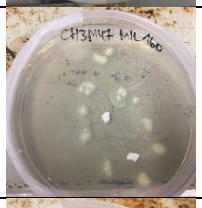	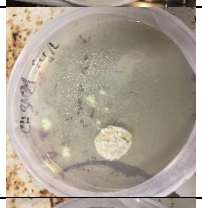	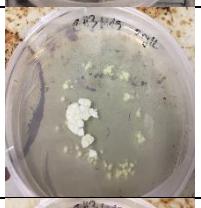	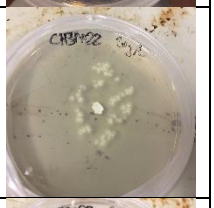
5				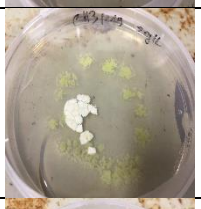	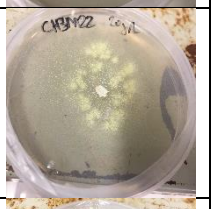
6					
11			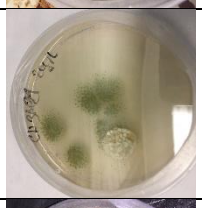	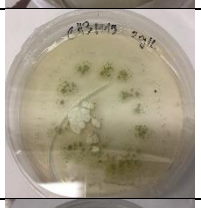	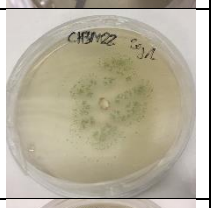
27			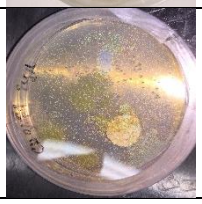		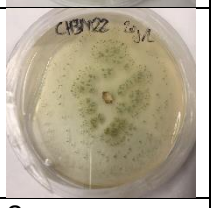
category	3	1	2	1	2

Sample / Day	Alfum@PVA	MIL-160@PVA	Alfum@ Silikophen®	MIL-160@ Silikophen®
0	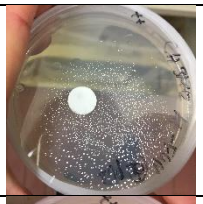	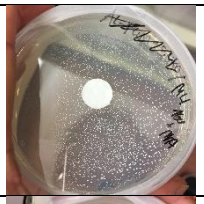	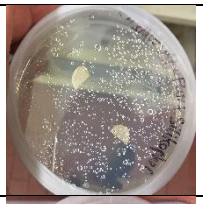	
2	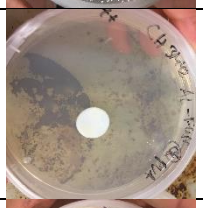	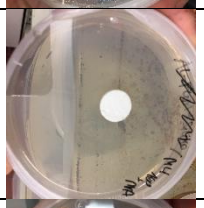		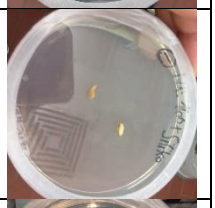
3				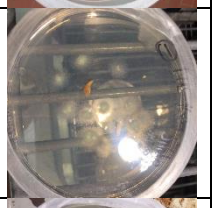
4		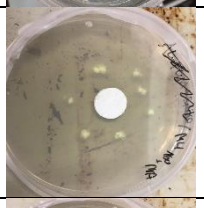	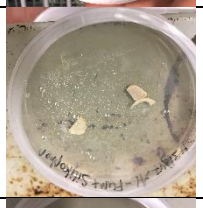	
5		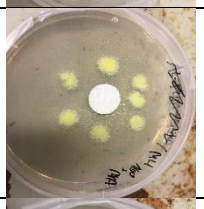		
6				
11	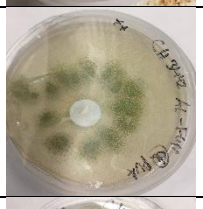	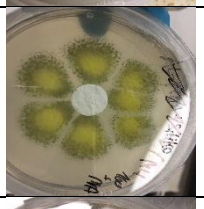	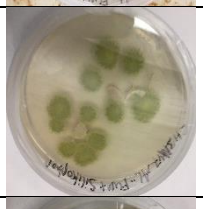	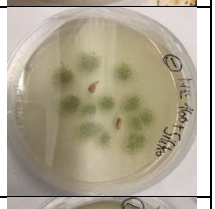
27	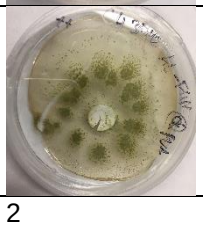	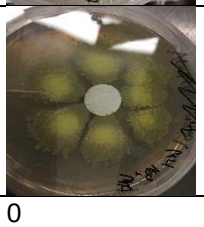		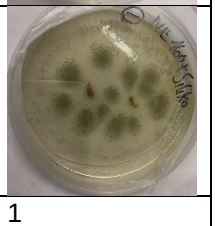
category	2	0	5	1

Method A: ***Aspergillus falconensis*** **(2./3. run, only final image after 30 days depicted)**

Sample / Day	Chitosan crosslinked	Alfum	Alfum60 @chitosan	Alfum80 @chitosan	Alfum90 @chitosan
30					
category	5	5	0	0	0

Sample / Day	Chitosan crosslinked	MIL-160	MIL-160(60) @chitosan	MIL-160(80) @chitosan	MIL-160(90) @chitosan
30		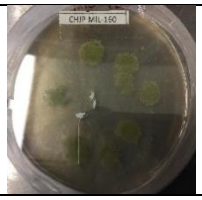			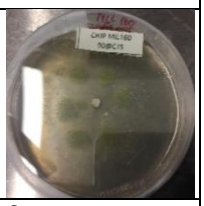
category	5	1	0	0	0

Sample / Day	Alfum@PVA	MIL-160@ PVA	Alfum@ Silikophen®	MIL-160@ Silikophen®
30			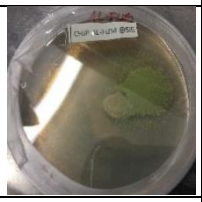	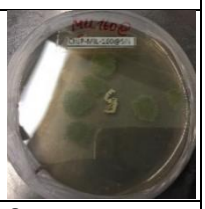
category	3	2	5	2

S12 Images of the MOF@chitosan composites

Images of the Alfum@Chitosan composites. Four exemplary selected beads.

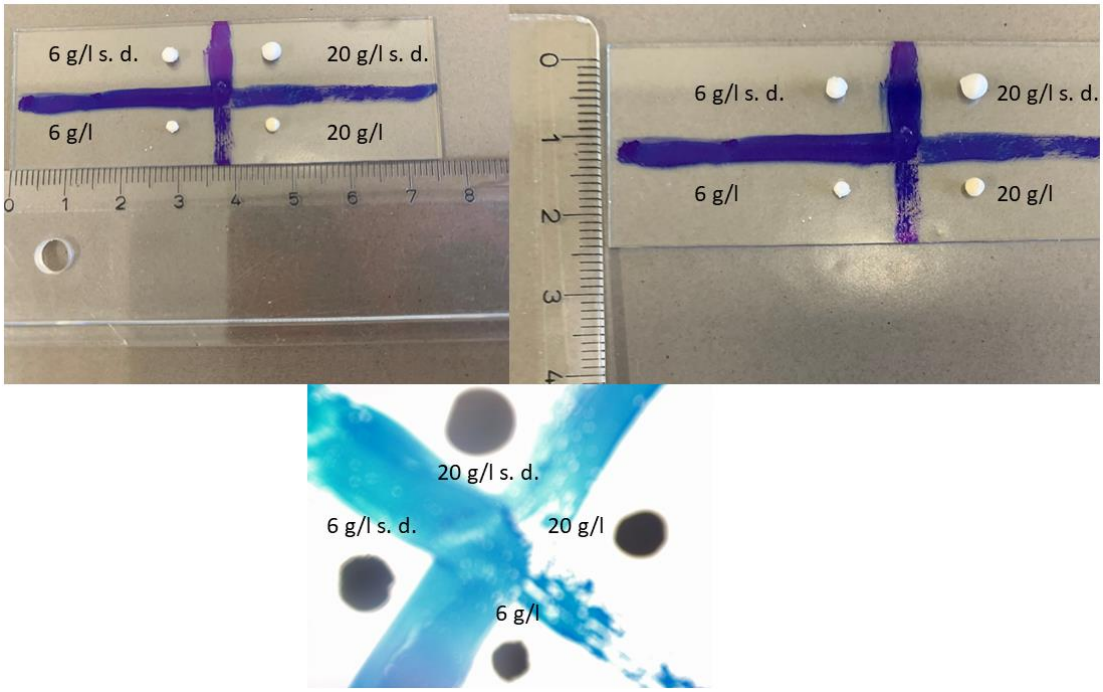

Figure S41: Images of the MOF@chitosan composites with camera (both images on top) and by a light microscope (below).

S13 Reaction scheme of chitosan and glutaraldehyde

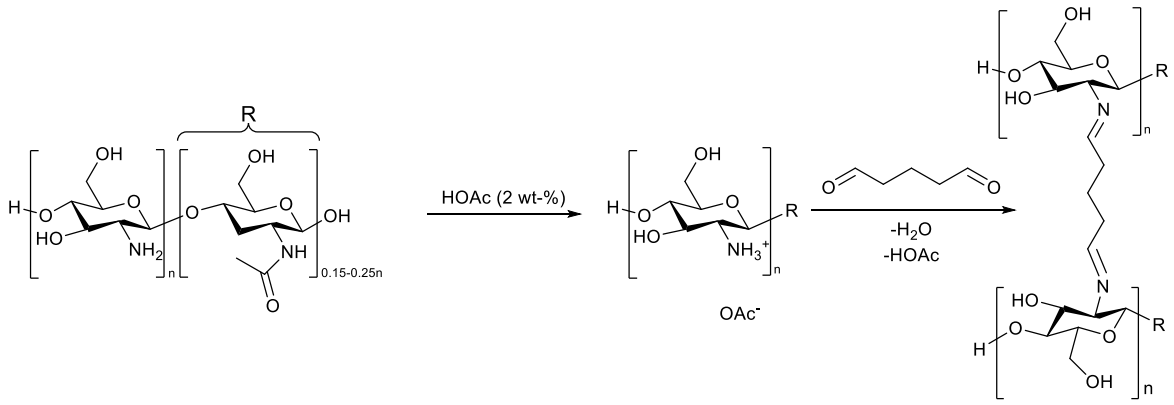

Figure S42: Reaction scheme of chitosan and glutaraldehyde.

S14 Graphics

S15 References

1 E. Leung, U. Müller, N. Trukhan, H. Mattenheimer, G. Cox and S. Blei, *Process for preparing porous metal-organic frameworks based on aluminum fumarate*, U.S. Patent No. 8,524,932, BASF SE, 3 Sep. 2013.

2 C. Kiener, U. Müller, and M. Schubert, *Method of using a metal organic frameworks based on aluminum fumarate*, U.S. Patent No. 8,518,264, BASF SE, 27 Aug. 2013.

3 K. Brandenburg, Diamond 4.6.6, Crystal and Molecular Structure Visualization, Crystal Impact - K. Brandenburg GbR, Bonn, Germany, 1997-2021.

4 Alvarez, E.; Guillou, N.; Martineau, C.; Bueken, B.; Van de Voorde, B.; Le Guillouzer, C.; Fabry, P.; Nouar, F.; Taulelle, F.; Vos, D. de; Chang, J.-S.; Cho, K.H.; Ramsahye, N.; Devic, T.; Daturi, M.; Maurin, G.; Serre, C. The structure of the aluminum fumarate metal-organic framework A520. *Angew. Chem.* **2015**, *54*, 3664–3668, doi:10.1002/anie.201410459.

5 Cadiau, A.; Lee, J.S.; Damasceno Borges, D.; Fabry, P.; Devic, T.; Wharmby, M.T.; Martineau, C.; Foucher, D.; Taulelle, F.; Jun, C.-H.; Hwang, Y.K.; Stock, N.; Lange, M.F. de; Kapteijn, F.; Gascon, J.; Maurin, G.; Chang, J.-S.; Serre, C. Design of hydrophilic metal organic framework water adsorbents for heat reallocation. *Adv. Mater.* **2015**, *27*, 4775–4780, doi:10.1002/adma.201502418.

6 Wahiduzzaman, M.; Lenzen, D.; Maurin, G.; Stock, N.; Wharmby, M.T. Rietveld Refinement of MIL-160 and Its Structural Flexibility Upon H_2O and N_2 Adsorption. *Eur. J. Inorg. Chem.* **2018**, 3626–3632, doi:10.1002/ejic.201800323.

7 Deutsches Institut für Normung. *DIN EN ISO 846 Plastics - Evaluation of the action of microorganisms;* Beuth: Berlin, 2018 (846:2018).

8 Thommes, M.; Kaneko, K.; Neimark, A.V.; Olivier, J.P.; Rodriguez-Reinoso, F.; Rouquerol, J.; Sing, K.S.W. Physisorption of gases, with special reference to the evaluation of surface area and pore size distribution (IUPAC Technical Report). *Pure Appl. Chem.* **2015**, *87*, 1051–1069, doi:10.1515/pac-2014-1117.